Characterization and Failure Analysis of Ceramic Filters Utilized

For

Emission Control During Coal Gasification

Final Technical Report

Work Performed Under Contract Number: DE-FG21-94MC31203--99

For

United States Department Of Energy

Federal Energy Technology Center

BY

Dr. Ziaul Huque, Dr. Daniel Mei and Dr. Jianren Zhou

Mechanical Engineering/Prairie View A&M University
College Of Engineering And Architecture
P.O. Box 397
Prairie View, Texas 77446-0397

TEL: (409) 857-4023 FAX: (409) 857-4395

March 1998

Abstract

Advanced integrated gasification combined cycle (IGCC) and pressurized fluidized bed combustion (PFBC) power system requires both hot gas desulfurization and particulate filtration to improve system thermal efficiency and overall performance. Therefore, effective high temperature ceramic filters are indispensable key component in both of the advanced IGCC and PFBC coal based power systems to perform hot gas cleanup work.

To meet the environmental particulate emission requirements and improve thermal efficiency, ceramic filters are mainly utilized to cleanup the hot gas particulate to protect downstream heat exchanger and gas turbine components from fouling and corrosion. The mechanical integrity of ceramic filters and an efficient dust cake removal system are the key issues for hot gas cleanup systems. The filters must survive combined stresses due to mechanical, thermal, chemical and steam attack throughout normal operations (cold back pulse cleaning jets), unexpected excessive ash accumulation, and the start up and shut down conditions.

To evaluate the design and performance of ceramic filters, different long term filter testing programs were conducted. To fulfill this purpose, two Advanced Particle Filter (APF) systems were complete at Tidd PFBC Demonstration Plant, in Brilliant, Ohio in late 1990 as part of the Department of Energy's (DOE) Clean Coal Technology Program. But the most undesirable thing ever happened was the sudden functional and physical failures of filters prior to its designed life time. In Tidd APF filter vessel, twenty eight (28) filters failed one time. Significant research effort has been carried out to find out the causes that led to the early failure of filters. In this work, the studies are emphasized on the possible failure causes analysis of rigid ceramic candle filters.

The objectives of this program were to provide an systematic study on the characterization of filters, material laboratory analysis on filter micro-structure, the dust cake dislodging mechanism and possible causes led to failures of ceramic filters. These research work includes 1) characterization on filter properties, 2) material laboratory investigation on cracked and un-cracked filter batches, 3) a thermal numerical simulation, 4) various physical testing on filter mechanical integrity and 5) the back pulse cleaning mechanism. These studies provide insights into variations of filter permeability, filter toughness against different mechanical loading impact, microstructure changes of filters, coal ash bridging and micro-thermal cracks induced during the cold back pulse cleaning process.

To characterize the physical properties of used and unused ceramic filters, filter permeabilities and the pressure field of the gas stream were measured within a filter chamber with the use of fast response pressure transducers and an automatic data acquisition system. Used filters displayed non-uniform permeability distribution along its axis; and these variations developed asymmetric flow pattern in the filter chamber.

Scanning Electron Microscopy (SEM) analysis was performed on filter surface topography to examine if there are changes in microstructure of the post run filters. X-Ray Photoelectron

Spectroscopy (XPS) was utilized for interfacial analysis on filters. X-Ray Diffractometer was also utilized to investigate filter micro-structure at molecular level and the arrangement of atoms and molecules on filter specimen. Material laboratory analysis indicates that the outer layer of used filters have different phase structure than its inner layers due to filtration of foreign materials.

Based on the thermal numerical simulation on the cold pulse back cleaning process, a sharp temperature gradient was developed as the cold pulse stream was injected into high temperature filter cavity. The large temperature gradient could have micro-cracks developed along the internal surface of the candle filter. However, back pulse induced micro-cracks can be reduced by providing heated back pulse stream to relieve the sharp temperature gradient developed within the filter.

According to the test data of various mechanical load testing performed on IF&P filters, these filters survived several simulated mechanical loading during particulate filtration process. The toughness of filter integrity indicates that dust cake dislodging mechanism plays a more important role in particulate filtration process.

Parametric studies were performed on back pulse dust cake dislodging process. Dust cakes, made of various materials and mixtures, were deposited on the external surface of the filter and dislodged with the use of back pulse cleaning. The build-up of dust cake on filter surface depends on the following factors: the type of particulate, particle size, cohesive forces between particles and particle to filter surface and the gas flow rate. To investigate the ash bridging problem, the filter surface was partially sealed as a simulation of partially plugged filter surface during particulate filtration process. The acquired test data confirmed that particulate could be agglomerate on top of the sealed filter surfaces; and these blind areas are difficult to be cleaned with multiple back pulse cleaning cycles.

According to the testing result, it concludes that an efficient dust cake removal system is one most important factor in helping prevent excessive dust cake deposition on filter surface. Poor cleaned filter surface areas could lead to ash bridging problem, which could be a possible cause contributing to the failures of ceramic filters. An efficient dust cake cleaning system can eliminate ash bridging and thermal induced load to protect filters from being damaged in the filter chamber.

Because of its high efficiency of an optimized back pulse cleaning system, the use of disposable metal oxide as an alternative of desulfurization sorbent during coal combustion or coal Gasification processes is feasible.

Disposable metal oxides can be injected into coal combustion or Gasification process to absorb corrosive chemical gases, including hydrogen sulfide. The very low cost of waste iron oxides and the elimination of the investment on sorbent regeneration could make it attractive to replace the regenerable sorbent candidates. Simultaneous particulate filtration and desulfurization will be feasible if the additional increase of dust loading of iron oxides can be successfully cleaned during the particulate filtration process.

Acknowledgements

The authors would like to thank the following individuals for project direction and guidance on this work: our Contracting Officer's Representative, Dr. Norman Holcombe, filter cluster leaders, Dr. T. K. Chiang and Dr. Duane Smith , and Mr. Charlie Komar as well as the management personnel at DOE/FETC. The authors also would like to thank mr. Robert Bradley and mr. John Nixon for their help and support in the loan of D.O.E. equipment to pV A&MU. Because of their extensive support and assistance on this research program, that made our visits to other research institutes and filter industries possible to understand more about particulate filtration industry and gain helpful technical advice. Special thanks to Mr. Komar for all the efforts and assistance provided in helping establish Hot Gas Cleanup (HGCU) research program and the test facility at Prairie View A&M University. Technical consultation and support provided by Westinghouse STC, Industrial Filter and Pump Manufacturing Company, and Southern Edison Company are gratefully acknowledged..

Research sponsored by the U.S. Department of Energy's Morgantown Energy Technology Center, under contract DE-FG21-94MC31203 with Mechanical Engineering/Prairie View A&M University, College of Engineering and Architecture, P.O. Box 397, Prairie View Tx 77446-0397; Tel: (409) 857-4023 Fax: (409) 857-4395

TABLE OF CONTENTS

	Page
List of Grafical Materials	7
Executive Summary	8
1.0 INTRODUCTION	10
1.1 Contract Objectives	10
1.2 Background	10
2.0 RESULTS AND DISCUSSION	12
2.1 Characterization of filter properties and filtration pressure field	12
2.1.1 Summary of characterization of ceramic candle filters	12
2.1.2 Discussion on particulate filtration testing	12
2.1.3 Description of particulate filtration test facility	13
2.1.4 Experimental procedures for characterizing ceramic filters	15
2.1.5 Results on characterization of ceramic filter properties	18
2.2 Material Laboratory Analysis on used and unused filters	20
2.2.1 Summary of material laboratory analysis	20
2.2.2 Experimental procedures	21
2.2.3 Results and discussion on material laboratory analysis	22
2.2.4 Conclusions of material laboratory analysis	24
2.3 Thermal Numerical Simulation On Back Pulse Cleaning	26
2.3.1 Thermal Analysis On A Single Filter With Cold Back Pulse	26
2.3.2 Recommendation On Future Thermal Analysis	27
2.4 Parametric Study On Back Pulse Cleaning Mechanism	28
2.4.1 Introduction on particulate filtration testing campaign	28
2.4.2 Key parameters affecting particulate filtration process	28
2.4.3 Study on dust cake dislodging via back pulse technique	30
2.5 Failure Analysis On Ceramic Filters	37
3.0 CONCLUSION	41
4.0 REFERENCES	42

List of Graphical Materials

Figure	Description
1-1	Schematic of IGCC and R&D Issues
1-2	Schematic of PFBC and R&D Issues
1-3	AEP candle filter failure locations
2-1-1	Schematic of candle filter and top sealing configuration
2-1-2	Schematic of filter test setup
2-1-3	Schematic of filter pressure field test setup
2-1-4	Schematic of section of filter and sensors location
2-1-5	Picture of filter test setup
2-1-6	Permeability variation of used filter (10) psi
2-1-7	Permeability variation of used filter (15) psi
2-1-8	Permeability variation of used filter (20) psi
2-1-9(a)	Permeability variation of unused filter (15) psi
2-1-9(b)	Permeability variation of unused filter (20) psi
2-1-10	Permeability circumferential variation of used filter (10) psi
2-1-11	Pressure sensor output of used filter (20) psi, outside filter
2-1-12	Pressure sensor output of unused filter (20) psi, outside filter
2-1-13	Pressure sensor output of used filter (5) psi, inside filter
2-1-14	Pressure sensor output of unused filter (5) psi, inside filter
2-2-1	SEM micrographs of unused, used and ultrasonically cleaned filters
2-2-2	SEM micrographs of unstable cracks penetration on inner and outer filter surface
2-2-3	SEM micrographs of the "river marks" through the outer layer of used filter
2-2-4	XPS spectra of the outer layer of the used and ultrasonically cleaned filter
2-2-5	XRD spectra of the layer formed by depositions and reactions on used filter surface
2-2-6	Picture of material laboratory analysis equipment
2-3-1	FEA model on filter back pulse cleaning near the neck with element meshing
2-3-2	Picture of FEA model on filter back pulse cleaning near the neck with element meshing
2-4-1	Schematic of test setup configuration for parametric study on filtration process
2-4-2	Configuration of back pulse gas stream setup for dust cake dislodging

EXECUTIVE SUMMARY

Advanced integrated gasification combined cycle (IGCC) and pressurized fluidized bed combustion (PFBC) power system requires both hot gas desulfurization and particulate filtration to improve power system performance and efficiency. To evaluate the design and performance of particulate filtration of ceramic filter system under high temperature and high pressure (HTHP), several long term filter testing programs were conducted. These programs included various testing performed by Federal Energy Technology Center at Morgantown since 1989 and the Tidd 70 megawatt (MW) pressurized fluidized-bed combustor (PFBC) Demonstration Plant, in Brilliant, Ohio in late 1990.

The twenty eight (28) pre-matured failures of the ceramic candle filters in Tidd Advanced Particle Filter (APF) attracted significant attention on the study of finding the possible causes that led to these filter failures. The objectives of this research program are dedicated to the studies on the characterization of ceramic candle filters, the fundamental mechanism of particulate filtration, dust cake cleaning with the use of back pulse, and the gas stream flow during particulate filtration process with the use of numerical simulation, material laboratory analysis and various mechanical loading testing on candle filters. A failure analysis was performed on the ceramic filters based on the test data acquired during this research program.

Due to the limit of testing facility and budget, the physical and mechanical properties of candle filters and particulate filtration testing were evaluated at room ambient temperature. Thermal finite element analysis was performed on the impact of cold back pulse steam to hot candle filter during back pulse cleaning to gain insights of thermal shock and temperature gradient along candle filter axis during back pulse cleaning. Material laboratory analysis was performed on both used and unused candle filters to characterize chemical and thermal attack induced on candle filters with the use of advanced equipment, including SEM and XRD analysis, during HTHP filtration process. Fast response micro-machined silicon pressure sensors were used with an advanced automatic data acquisition, developed with the use of the graphical programming LabVIEW provided by National Instruments, to study filter permeability variations along external filter surface and the gas stream pressure field in the filter camber during particulate filtration process.

The candle filter manufacturers has made significant progress in the improvement of filter physical and mechanical properties. Most of the filters developed by different suppliers are able to meet the thermal and mechanical requirements for HTHP operation environments. At Prairie View, IF&P candle filters survived high G level vibration, acceleration and shock impact testing performed on candle filters.

Significant effort was dedicated to the study of the back pulse cleaning of different dust cakes developed on filter surface. A parametric testing was performed on the pulse strength, the size and location of the back pulse jet to gain insight of dust cake dislodging mechanism. Dust cake materials include flour, coal ash originating from the Curtis-Wright PFBC facility, and their

mixtures with iron oxide. based on the test data, it appears that an efficient back pulse cleaning system is one of the key factors to the success of particulate filtration process.

To gain insights of dust cake cleaning mechanism, candle filter surface had been partially sealed to simulate plugged areas scattered on external filter surface during particulate filtration testing. Test data indicates that particulate did accumulate on top of the plugged areas after performing many cycles of dust cake development and back pulse cleaning.

A failure analysis was performed based on the test data acquired and concluded with the use of the process of elimination. It seems that the lack of a high efficient back pulse cleaning system and plugged areas on the filter surface would be the primary causes led to coal dust cake bridging. The uneven dust cake cleaning power distribution and the failure of filter mechanical integrity would also contributed to the loss of back pulse cleaning power.

1.0 INTRODUCTION

1.1 Contract Objectives

The objectives of this work were to characterize the physical properties of ceramic candle filters utilized for hot gas particulate cleanup, to study the mechanism of particulate filtration process and to perform a failure analysis based on the research work of material laboratory analysis, thermal numerical simulation results and the test data acquired in this contract work.

The scope of work in this research program included the following:

- Characterization of candle ceramic filter properties; and the pressure field within a filter testing chamber during filtration operation;

- Material Laboratory analysis on used and unused filters;

- Conducting thermal numerical simulation on candle filters during hot gas cleanup;

- Evaluation on current dust cake dislodging method - back pulse cleanup mechanism;

- Investigating of candle filter integrity by various mechanical loading testing;

- Performing a failure analysis on candle ceramic filters.

1.2 Background

Electricity demand has been closely tied to economic growth. The need for electrical power is estimated to double for every twenty years. Advanced energy conversion systems, include the integrated gasification combined cycle (IGCC) and pressurized fluidized bed combustion (PFBC) are attractive for power generation (schematic of IGCC and PFBC and its research issues are shown in **Figure 1-1 and 1-2**), because it can improve the thermal efficiency of electricity generation with low capital and operating costs. However, IGCC and PFBC power system requires both hot gas desulfurization and particulate filtration to improve power system performance, protect high temperature gas turbine system, heat exchange components from corrosion and damages caused by gasified particulate, and meet the clean air environmental protection measures.

Hot gas cleanup is one of the most critical technologies required to ensure the success of low-cost methods of electric power generation. Ceramic filters are indispensable in removing the particulate in coal gasification applications. The mechanical integrity of ceramic filters and an

efficient dust cake removal system are the key issues to be resolved for hot gas cleanup systems. The filters must survive combined stresses due to mechanical, thermal, chemical and steam attack throughout cold back pulse cleaning jets and system start up and shut down conditions.

Among the current hot gas cleanup technologies, the most economical one is the use of rigid ceramic candle filters and the back pulse cleanup technique to remove dust cake to filtrate high temperature and high pressure particulate from gas streams.

To evaluate the design and performance of ceramic filters, different long term filter testing programs were conducted. To fulfill this purpose, two Advanced Particle Filter (APF) systems were complete at Tidd PFBC Demonstration Plant, in Brilliant, Ohio in late 1990 as part of the Department of Energy's (DOE) Clean Coal Technology Program. But the most undesirable issues ever happened were the sudden functional and physical failures of filters prior to its designed life time. In Tidd APF filter vessel, twenty eight (28) filters failed one time (AEP candle failure locations are shown in **Figure 1-3**).

Significant research effort has been carried out to find out the exact causes of early failure of filters since the failures occurred. Since then, researches were emphasized on the improvement of the physical and mechanical properties of ceramic filters. And significant progress were made to enhance the current filters survive 800 degree C operation temperature without losing the toughness and the mechanical strengths of candle filters. However, less study was performed on the particulate filtration and dust dislodging mechanism. Therefore, more attention was concentrated on the changes of filter properties and back pulse cleaning mechanism in this study to resolve the issues relating to filter permeability variations, ash bridging and micro-thermal cracks induced during cold back pulse cleaning.

In this work, the studies are emphasized on the characterization of candle filters, the dust cake dislodging mechanism, the evaluation of the back pulse cleaning parameters and the failure analysis of rigid ceramic candle filters.

2.0 RESULTS AND DISCUSSION

2.1 Characterization of filter properties and filtration pressure field

2.1.1 Summary of characterization of ceramic candle filters

To study particulate filtration phenomena, a particulate filtration test chamber was built to characterize properties of ceramic candle filters. To facilitate the testing and observation of dust cake deposition on candle filter, the particulate flow pattern and filter properties, a cold flow simulation on particulate filtration flow was investigated within a transparent filtration chamber. Many valuable test data were acquired through the study of cold flow simulation of particulate filtration process.

Comparison of filter permeability variations along ceramic candle filter surfaces, caused by field test operations, were illustrated by the measurement of the flow resistance through the used and unused filters within the test chamber. To gain insights into the gas flow pattern during particulate filtration process, the pressure field distribution within a filter testing chamber was also measured for both used and unused filters.

To facilitate the measurement of the variation of the pressure field within filter internal cavity and the filter chamber, small size and fast response pressure silicon micro-machined pressure sensors were utilized. An advanced data acquisition programming was developed for the data acquisition hardware procured from National Instruments to interface with various instruments via RS 232, RS 485 and IEEE 488 to perform data acquisition task.

Because of the random distribution of filter permeability of the used filters, a non-uniform pressure distribution field was generated in the filtration test chamber designed with a cylindrical symmetry configuration. The asymmetric pressure field developed a reversed gas flow as the filtration gas stream flew through the filtration chamber throughout the filtration simulation testing. The non-uniform flow pattern suggested that the pressure distribution along filter axis may not be uniform as the back pulse jet entered into filter cavity during back pulse cleaning process. This uneven jet pulse pressure distribution might develop uncleaned dust patches along the filter surface and enhanced the growth of the dust cake as the filtration process proceeds in the field.

2.1.2 Discussion on particulate filtration testing

Prior to the design of the filtration chamber, literature survey, selection of filter samples and filter characterization test plan were conducted.

Extensive literature survey was performed on particulate filtration research work conducted by academic and industrial researchers. Most of these filtration work were concentrated on filter microstructural or material studies, mainly on investigation of mechanical, thermal and chemical properties of filters. Westinghouse and South Research Institute has performed significant amount of testing work on the thermo-mechanical properties of various filters supplied by filter industry. But little work had been concentrated on the study of variations of filter permeability and the pressure distribution field of the gas stream during dust cake cleaning process. Therefore, a transparent filter chamber was designed and built for candle filter filtration study. Significant effort was provided to develop an automatic data acquisition system via the use of LabVIEW graphical programming procured from National Instruments. The test software and instrumentation interfacing programming was installed in a personal computer (PC) controlled by Window management. The PC based data acquisition system help collect pressure sensor outputs automatically and interfaced with Excel spreadsheet for test data post processing. A test plan was generated to study the variations of filter permeability and gas flow pressure field in the filtration chamber.

It was difficult to select adequate filter samples for filter characterization testing, because there were advantages and disadvantages of testing the failed filters vs. the improved filters. To perform a formal failure analysis, the failed filter batches shall be selected and failed sample pieces needs be thoroughly analyzed; and the failed symptoms needs be duplicated with proposed failure causes. Because the limit of the budget, manpower and test facility, it is difficult to repeat the test operations to simulate the test operation environments. Meantime, the filter suppliers were making significant progress on filter performance improvement since the filter failures, the testing on old and less matured filters would not help predict the performance of recently developed filter candidates.

After a thorough discussion between filter research group at PV A&M University and the Federal Energy Technology Center (FETC) management, the filter samples for this analysis program were selected to be the silicon carbide ceramic filters supplied by Industrial Filter & Pump Company (IF&P), located at Chicago, Illinois, U.S.A.. These filters' dimensions are 100.00 cm (39.37 inches) long, 3.81 cm (1.50 inches) I.D. and an O.D. of 6.35 cm (2.50 inches).

2.1.3 Description of particulate filtration test facility

The schematic of the candle filter and the filter sealing configuration for room ambient temperature filtration testing is shown in **Figure 2.1.1**. Beside a ceramic candle filter, the filtration test facility consists of a transparent filter test chamber, an automatic data acquisition system, a set of macro-machined silicon pressure sensors, a set of pressure source supply and instruments for pressure control.

To facilitate the testing, this test chamber vessel was made from a transparent plastic pipe with a 15.24 cm I.D. (6.00 inches), 198.12 cm (78 inches) long and 0.71 cm (0.28 inches) wall

thickness. This filtration vessel passed a 10.2 bars (150.0 psig) static pressure testing, compatible with Tidd APF pressure level, prior to its final assembly. Ten 1/2 - 20 threaded holes are evenly spaced along the chamber axis to mount fast response pressure transducers and the test port for an advanced pressure calibrator.

The output of the pressure sensors can be connected to the PC based data acquisition system or interfaced with the advanced pressure calibrator. The pressure calibrator has two ports for different sensing modules, and the output display can be configured with different units for ease of operation and data management. The pressure sensor outputs can be monitored real time with the use of the advanced pressure calibrator; therefore, the pressure calibrator was utilized when the real time pressure reading was required.

A filter sealing plug base of 15.33 cm (6.03 inches) diameter by 8.90 cm (3.50 inches) long and a pressure inlet plug with the same exterior dimensions are installed one at the top and one at the bottom end of the test chamber respectively. All the machined parts of the test chamber were fabricated with a tight tolerance control of +/- 0.002 inches to ensure air tight sealing throughout the filtration testing.

The ceramic candle filter was installed in a multiple pressure sealed assembly to ensure the hermetic sealing between the machined parts and the filter chamber, between the filter and the machined parts and between the filter and the filtrated gas stream plenum assembly. Silicon sealing grease was applied between all the machined parts and the interfaced filter sealing areas to enhance the hermeticity sealing and capture the unfiltered particulate if any throughout the filtration testing. This design assembly was filtration tested with maximum testing pressure and the test results confirmed that no particulate could be carried with the filtrated gas stream outside the filter as long as the filter performs particulate filtration successfully.

The candle filter was located at the center of the pressure sealing assembly. The alignment of the filter axis and that of the filter testing chamber equipped the filtration test system with a configuration of cylindrical symmetry. To reduce shock impact and mechanical stress on the filter flange during filter installation process and filter particulate filtration testing, properly designed elastomer pads were installed within and between the filter and the sealing plug assembly.

A pressure sealing diaphragm was initially installed on the top of the filter sealing assembly to develop a pressure control device and a shock tube type testing setup for the preliminary filtration testing. The sealing diaphragm was perforated by a specially designed perforating device to establish the chamber pressure per the ambient pressure test plan. **Figure 2.1.2** shows the schematic of the diaphragm perforating arrangement. As the filter chamber was pressurized to the preset testing pressure, the pressure sealing diaphragm was then perforated to generate a controlled gas stream. The pressure distribution history of the controlled gas stream was recorded as a correlation measure to characterize the filtration properties of ceramic filters.

A fast response solenoid valve with a quick close and opening response time, less than 700 milliseconds, was utilized to replace the sealing diaphragm after the characterization testing of filter filtration properties was complete. The fast response solenoid valves were also utilized for dust cake dislodging testing. The instaneous opening of a normally closed fast response solenoid valve helped generate a high speed pressure jet pulse for dust cake removal testing as required by the back pulse cleaning technique.

2.1.4 Experiment procedures for characterizing ceramic filters

The objectives of this subject testing on filter properties characterization are to measure the variations of filter permeability on used and unused filters and evaluate the pressure field distribution within the filtration chamber as filtration process proceeds.

Most of filter suppliers measure filter permeability with a lumped sum average value for the entire filter. However, this lump-sum measurement can not identify the changes of filter permeability along filter surface. Therefore, the filter permeability distribution was measured with a partially exposed filter surface each time for used and unused filters in this subject testing. A innovative technique was developed to seal the unexposed filter surface areas when the filter permeability was evaluated. As expected, the test data proved that the used filter permeability distribution had been changed randomly after coal power plant demonstration testing.

The pressure field distribution within the filtration chamber was measured with the use of micro-machined silicon pressure sensors installed along the chamber wall paralleled to the axis of the filtration chamber and installed within the filter cavity as a clean stream of pressurized nitrogen flew through the filtration system. The test setup and the picture of assembled filtration test system are shown in **Figure 2.1.3, 2.1.4 and 2.1.5**. The reason that the clean nitrogen was used to measure the pressure field distribution in the filtration chamber is to eliminated the pressure resistance could be caused by the particulate deposition on filter surface during the testing process. The clean nitrogen flow will help identify the pressure field distribution with the use of fast response silicon pressure sensors and an adequate data acquisition system.

Before each testing, the pressure sensors were carefully calibrated and each testing was repeated five times to ensure that the test data were repeatable and reliable.

2.1.4.1 Characterization of filter permeability variations on ceramic candle filters

To characterize the variations of filter permeability on used and unused filters, a technique had been successfully developed to seal part of the filter surface as the filtration gas stream flew through the rest of opened areas on the filter surface. This technique was tested proved over the entire external filter surface area first to ensure the sealing design was 100% hermetic. After the sealing test, this technique was utilized to characterize the distribution of filter permeability along the tested filter axis and its perimeter.

To facilitate the testing of filter permeability characterization, the filter surface was divided into four different areas along its axis for filter permeability measurement, section to section. For each 1/4 length section of the filter, the section area was also divided into four equal regions for permeability evaluations. Each selected 25% of the filter surface area, both along filter axis and its perimeter, was evaluated with the same test setup and the same test environment.

The differential pressure (Delta P), measured from within the filtration chamber and the filtrated gas plenum, was normally measured as the lump-sum filter flow resistance. The Delta P is an averaged value of filter resistance to the filtration gas stream, it is very informative to identify the increase of dust cake deposition on filter surface during the filtration process. But Delta P can hardly tell the distribution of the plugged areas along the filtration filter surface when Delta P value increases during filtration process. Another difficulty of using Delta P to measure filter permeability distribution is the very low pressure differential value, typically 2.5 inches of water column, measured across a cleaned filter. And the Delta P value across a 25% of the entire filter surface and the 1/4 of the perimeter of a 25% long filter section would be even lower. These very low pressure differential values would be more difficult to measure with the resolution of a 30 psig range pressure sensors, mounted on the wall of the filtration chamber.

However, an opened section along the filter surface can be independently evaluated with a preset test environment. The distribution of filter permeability can be identified with the isolated permeability evaluation testing, piece by piece. The variations of filter permeability were displayed after test data post processing through permeability variation plotting.

To overcome these difficulties for filter permeability characterization, an innovative test plan was designed to measure the permeability distribution indirectly. The test philosophy is to measure the elapsed time required for a pressurized filtration chamber to release the sealed gas stream out of the filtration chamber through each open section of the filter exposed to the sealed pressure reservoir. The time history required for each tested filter section would provide a relative index to the flow resistance of the filter section tested.

The total period of time required for preset positive gas pressure, sealed within the filtration chamber, to reduce to room ambient pressure was recorded and used as a relative measure to correlate the permeability variations of the filters evaluated. The test data revealed that the unused filter is characterized with a uniform permeability distribution, but the used filters is characterized with random variation of filter permeability throughout external filter surface. Positive pressure source was provided by nitrogen gas bottle throughout the permeability characterization testing.

The permeability test procedures are summarized as follows:

(1) Select an open area for filter permeability characterization; seal the rest of filter areas along the external filter surface.

(2) Install the partially sealed candle filter into the pressure sealing assembly of the filtration chamber.

(3) Power the pressure sensors and turn on the data acquisition system to warm it up for 30 minutes prior to the testing.

(4) Pressurize the filtration chamber to a preset pressure range and isolate the pressure source to the gas stream entrance port on the filtration chamber.

(5) Perforate the pressure sealing diaphragm, installed on the top pressure sealing assembly of the filtration chamber, with the use of the diaphragm perforating device to release the sealed pressure reservoir to the ambient pressure level.

(6) Set the timer and data acquisition system to zero and record the elapsed time interval with the corresponding pressure reading of the flowing gas stream confined in the filtration chamber.

(7) Repeat step (6) until the chamber gas pressure reached to the ambient pressure.

(8) Evaluate the test data for its repeatability. Repeat test procedures from step (4) to step (8) for another four times if the test data are repeatable. Stop the testing and find the problems. Correct the errors and proceed the testing as required.

(9) Stop the testing and dis-assemble the test setup and prepare for the testing of the next selected filter section area. Repeat the entire test procedures when the test setup is ready.

During filter permeability characterization testing, five tests were performed for each pressure range and the test data were reviewed to ensure it were consistent and repeatable. Because of the test data were highly repeatable, the average values of test data were used for permeability variation plotting to make the plotting easy to read. Because the high repeatability of the test results, the averaged test data still represents the characteristics of filter performance with good confidence.

2.1.4.2 Characterization of pressure field within filtration chamber

To characterize the pressure field within the filtration chamber during filtration process, the static pressure reading at different locations along the filtration chamber wall were measured as nitrogen gas flew through the entire filter surface. Pressure sensors were utilized with a data acquisition system to investigate the pressure field within the filtration chamber as the gas stream flew through the filtration system. Based on the test data of filter permeability characterization testing, the unused filter is characterized with a uniform permeability distribution. Therefore, an used filter was evaluated in the filtration to characterize the pressure field as filtration proceeds in the field.

Several pressure sensor candidates were evaluated to perform the testing. Pressure sensors will be installed along filter axis both inside and outside tested filter. Due to the constraint of the small size of filter I.D. (1.50 inches) and the requirement of not to disturb the flow pattern with the insertion of the sensor within the filter cavity, sensor size and response time are critical factors for sensor candidate selection. The micro-machined silicon pressure sensor cell and its silicon pressure transducer are characterized with fast response time and small size, so it were utilized to acquire pressure readings throughout the entire testing program. Silicon pressure transducers, with 1.0 inch O.D. and 1/2-20 threaded pressure port, were mounted on the filtration chamber and silicon sensor cell with 9/16 inches O.D. was installed into filter cavity for pressure field evaluation both inside and outside the candle filter.

Ten micro-machined silicon pressure sensors are mounted along one side of the filtration chamber, equally spaced along the axis of the chamber. The outputs of ten pressure sensors were recorded and compared with the reference pressure of inlet gas stream to characterize the pressure field outside the candle filter. The deviations of the pressure readings compared to the reference pressure were utilized to characterize the pressure field within the filtration chamber during particulate filtration process.

During the testing of chamber pressure field, the inlet gas stream pressure was monitored continuously; and the pressure outputs of the wall mounted transducers were recorded by the data acquisition system. The output deviation between the reference pressure and the transducers were plotted as a measure of the pressure field in the filtration chamber. Based on the test data, it appears that a non-uniform pressure field was detected as the gas stream flew through the used filter. Reversed gas stream flow were also observed during the testing at few sections along the filter axis.

With the pressure sensor installed within the filter cavity at different locations along filter axis, the pressure readings of the sensor would provide the researchers with the pressure field within the filter. As the sensor cell was installed at different positions along the filter axis, the pressure readings were recorded in the same steps as the exterior pressure field testing. It was interesting to find out the pressure distribution within the filter varies in the similar pattern as the exterior field does. These test data would help understand the behavior of the gas stream within the filter during the filtration process.

2.1.5 Results on characterization of ceramic filter properties

To ensure the reliability of the test data, every test was repeatedly performed five times, and the test results were found repeatable and consistent.

2.1.5.1 Results on filter permeability characterization

The filtration chamber pressure distribution vs elapsed time measured per the test plan with an unused and used filter were shown in **Figure 2.1.5, 2.1.6, 2.1.7, 2.1.8, and 2.1.9**. As shown in the test results, the pressure deviations of the four different sections along the filter axis were negligible. The same test results were also observed for the circumferential permeability evaluation (shown in **Figure 2.1.10**). It can be concluded that the filter permeability of an unused filter is uniform along the entire filter surface.

On the contrary, for used filter, the pressure deviations of the four different sections along the filter axis were significant. These pressure deviation was worse as the chamber pressure increased. This phenomena was consistent with the finding that filter resistance to filtration gas stream increased with filter face velocity. Reversed gas flow were observed as clean nitrogen flew through the used filter. Similar pressure deviation pattern was observed within the filter cavity.

As shown in Figure 2.1.10, filter permeability also varies in the circumferential direction. It can be concluded that the filter permeability of an unused filter is non-uniform along filter axial and circumferential direction. The variations of the permeability of the used filter was characterized with a random distribution pattern.

The changes of filter permeability from an uniform pattern of an unused filter to a non-uniform one shown on an used filter indicated that the changes were caused by the field testing processes and the testing operation environment.

It can be concluded that the filter permeability will be affected by the operation history of the used filter. Every filter will experience combined attack of mechanical, thermal, chemical and back pulse loadings during the filtration process. These critical loading and the efficiency of the back pulse cleaning system are causes that changed filter properties.

2.1.5.2 Results on pressure field characterization within filtration chamber

The outputs of pressure transducers mounted on the chamber wall is shown in **Figure 2.1.11 and 2.1.12**. The outputs of the pressure sensor cell inside the filter are shown in **Figure 2.1.13 and 2.1.14**. The pressure outputs crossed over each other as an evidence of pressure fluctuations experienced during the filtration process. Based on the pressure outputs measurement, it showed that the pressure field within the filtration chamber was non-uniform both inside and outside the filter cavity.

The non-uniform pressure field detected through this testing was consistent with the finding of the random variations of the permeability of an used filter. The filtration properties of filters would be changed by the dust loaded gas stream, these changes converts the particulate filtration system into a non-uniform and dynamic one.

2.2 Material Laboratory Analysis on used and unused filters

2.2.1 Summary of material laboratory analysis

Ceramic candle filters have been extensively used in the filtration of coal derived gases at high temperature and pressure. However, due to severe working condition and environment, some filters deteriorated prior to the desired life time. It is very important to identify and investigate the filter degradation mechanisms.

Material Laboratory analysis on used and unused filters is to provide a thorough study on ceramic filters. Theoretical analysis and material laboratory investigation were performed on cracked and un-cracked ceramic filter batches to identify the causes of filter failures. Scanning Electron Microscopy (SEM), X-Ray Photoelectron Spectroscopy (XPS), and X-Ray Diffractometer (XRD) were performed on used and unused filters.

The used and unused filter samples were characterized for various properties; including surface topography, microstructure, surface chemical composition, percentage chemical composition, chemical binding state and crystal structure.

The sample filters were made of silicon carbide (SiC), and it had been tested under the following conditions:

- Gas temperature: 650 degree C;
- Gas pressure: 20 kg/cm2;
- Face velocity: 5 - 10 cm/sec;
- Jet pulse pressure: 35kg/cm2;
- Jet pulse duration: 1.0 second;

Surface topography and micro-structure of fractured surface of ceramic filters were examined by using SEM to identify whether changes in microstructure of the post run filters have been occurred and how it affect the function and durability of the ceramic filters.

XPS was utilized for interfacial analysis of the filters. XPS is a highly surface sensitive technique in measuring the kinetic energy and the bonding energy of the electrons in the filter surface. Percentage of chemical composition and chemical binding state of ceramic sample were obtained with the use of XPS. The chemical shift of the detected electron serves to identify the contained chemical species in the filter. The structure composition of a filter as a function of depth could be identified via the use of ion sputtering and angle resolved XPS techniques. Angle resolved XPS helped to characterize the filter composition distribution over a small depth change.

Molecular structure and crystal constant was obtained by XRD method. XRD was also utilized in the present work to investigate the micro-structure at the molecular level and the arrangement of atoms and molecules in various phases of the ceramic filter specimen. The test data were automatically collected via a personal computer based data acquisition system, and they were statistically analyzed and documented.

2.2.2 Experimental Procedures

2.2.2.1 Scanning Electron microscopy (SEM)

The micro-features and surface topography of ceramic filter samples (used and unused) were primarily analyzed by SEM. These samples were cut into square pieces in size of 1cm x 1cm. They were then sputtered with gold coating on a Tectonics Hummer Sputter Colter. The samples were mounted on a 3/8 inches aluminum tube with double stick tape, and carbon paint were then loaded in vacuum chamber of JEOL JSM 6400 SEM. The SEM is equipped with digital imaging system to enhance the appearance of the image directly on the microscope, thus gives the potential for better resolution. The image processor also allows the operator to do gray-scale manipulation and gamma correction.

SEM tests were performed by an Amary 1610 Turbo Microprocessor Controlled SEM. The AMARY 1610 SEM has a maximum magnification up to 400,000 X at 12 mm working distance thus providing insight into the microscopic structure that otherwise would not be possible.

2.2.2.2 X-Ray Photoelectron Spectroscopy (XPS)

Samples were mechanically cut to produce thin samples. These samples were clipped under gold plated clips in a surface science SSX-100 ESCA instrument (ESCA = Electron Spectroscopy or Spectrometer for Chemical Analysis). The instrument used a mono-chromatized Al k-alpha x-ray (1486.6 eV) for excitation. By providing digital beam control of the 6400, this system also facilitates multiple element x-ray mapping and scan analysis as well as image processing and storage. The user can store chemical and image data either on removable discs or on high-capacity tape streamers. The characterization is performed by measuring the peak x-ray produced when an electron-beam hits a target material, identifying each element presented by the characteristics of wavelength of its x-ray, and measuring its concentration by the number of x-ray photons produced per second. The carbon 1s line is used as a reference point in the analysis and a flood gun (low energy electron beam) was used to correct for electrostatic charging as necessary.

2.2.2.3 X-Ray Diffraction (XRD)

The samples that were used in XRD were similar to those used in XPS. The samples were mounted on aluminum base with double stick tape in the XRD chamber. XRD consists of an X-ray generator, a goniometer and a sample holder, and an X-ray detector such as photographic film or a movable proportional counter. X-ray tubes generate X-rays by bombarding a metal target

with high-energy (40Kev) electrons that knock out core electron. An electron is an outer shell fills the hole in the inner shell and emits an x-ray photo.

2.2.3 Results and discussion on material laboratory analysis

2.2.3.1 Morphological Examination of ceramic filter Samples by SEM

The micro-features and surface topography of unused, used, and used but ultrasonically cleaned ceramic filter samples were primarily analyzed by SEM. The results of the SEM showed that the unused ceramic filters have porous microstructural features, and the dimensions of the pores are about several ten micrometers with no fractured or broken surface. As for the used filter, the SEM pictures revealed broken and fractured surfaces in the inner and the outer layer due to thermal stress induced by cold back pulse cleaning and structural stress caused by thermal volume expansion. Also, traces of particulate and ashes were found in both layers of the used filter samples.

The micrographs of used (with or without ultrasonically cleaning), and unused filter samples are presented in **Figure 2.2.1**. The pictures show that the micro-structure of the filter can be divided into three regions. The first is the outer layer with a fine microstructure feature which correspond to aluminosilicate membrane of ceramic filter. The inner layer with coarse grains represents the support matrix (clay-bonded silicon carbide) of the ceramic filter. The third one is the interfacial region between the first and second layer. In this region, the microstructural characteristic transforms from one to another, i.e., from fine to coarse. Although there is no abrupt transition in the interfacial microstructure, the differences of microstructure features in the inner and outer region are easily to be differentiated. The outer layer has a porous cotton-like microstructural features, and the dimensions of the pores are about several ten micrometers. In the inner layer, with a porous microstructure too, the grains with several ten micrometers in size are bonded by clay and the pores are generally formed at the boundaries between the grains.

For the used ceramic filter, the volume expansion generated by the changes in microstructure of the grains might induce stress fields inside in the filter matrix, which would further promote the nucleation and propagation of the micro-cracks at some inclusions and defects sites leading to the fatigue fracture failure of the ceramic filter. the inconsistency in changes of crystal constants and structure between inner and outer layer would cause delimitation of the ceramic filter structure. The unused filter usually have a fine coherence between inner and outer layer, while the used filters show that some particles have been dropped off the interfacial region. In addition, the growth of grain and volume expansion of the used filters may lead to the reduction of volume ratio of the pores, and a s a result, decrease the permeability of the ceramic filters.

Observation of the post-run filters also show that there are numerous cracks developed on the surface of the failed ceramic filter and **Figure 2.2.2** displays a typical example of the defects. Some of them first initiated along the longitudinal direction, and then developed in about 45

degree away; and finally intersect with each others and caused fracture failure of the ceramic filter.

One of the failure experienced by tested filters was the shear failure of the filter close to the top end of the filter, which was clamped to the tube sheet within the filter vessel. During the particulate filtration process, it was difficult to clean out all of the dislodged particulate including coal ash and spent sorbent, etc. from the bottom hopper. If the back pulse cleaning system was unable to 100% dislodge the dust cake deposited on the filter external surfaces, residual dust cake would be left on the uncleaned filter areas. These dust patches would grow with time as more particulate kept depositing on top of the residues and experienced less cleaning power to have the growing patches removed. Therefore, the filtration system turned out to be dynamic system with time. These dust patches might grow and inter-connect with the adjacent patches and ash bridging was then developed within the filter chamber.

Ash bridging and the increasing particulate loading the filter vessel could eventually filled most of the space within the filter chamber when the back pulse cleaning and dust removal from hopper was not efficient. The thermal mismatch and the heavy weight of the uncleaned dust in the filter vessel could develop a severe mechanical loading to the filter clusters as the system went through a large temperature gradient, such as the shut down of the filtration system for inspection. The large and random mechanical load applied to the filters could deform the filters, because the filter physical strength reduced significantly at high operating temperature. The hot soft filter matrix would yield to the external thermal and mechanical loads caused by excess hot dust loading. The interface of the piled dust and the free space generated a sharp stress concentration areas to filters in the filter vessel. These stressed filter areas would experience more and more mechanical load as the filter vessel temperature cooled down to room ambient temperature. This unexpected thermal induced stress could induced filter failures close to the top end of the filter as they were clamped to the tubesheet, the severe shearing load caused by a large displacement on the filters but with clamped ends in the tubesheet would be responsible for the shear failures of the filters. As shown in **Figure 2.2.3**, cleavage fractures developed near the top section of the used filters are evidence of filter damage displayed from the inner layer expanding to the outer layer.

2.2.3.2 Surface Analysis of filter samples by XPS

The outer and inner layers of the unused filter, used, and used but ultrasonically cleaned filters were examined by XPS. Survey scans were collected from each surface and analysis was made to determine surface compositions. High resolution carbon, oxygen and other elements spectra were collected from all surfaces which did not exhibit severe charging and for which the elements level were high enough to give meaningful results.

The spectra in **Figure 2.2.4**, as an example of XPS spectrum, indicates all elements presented in the outer layer of the used filter cleaned by ultrasonic showing the presence of elements of carbon, oxygen, calcium, iron and silicon. Analysis of the atomic concentration and binding

energies of the elements presented in the outer layer on the used filter cleaned ultrasonically shows 29.4% - 292 for carbon, 49.2% - 30 for oxygen, 5.4% - 444 for calcium, 1.8% - 1074 for sodium, 0.4% - 715 for iron, and 13.3% - 158 for silicon, respectively. Analysis of the results of the inner layer of the used filter ultrasonically cleaned showed that the atomic concentration and the binding energies of 38.0% - 291 for carbon, 47.0% - 29 for oxygen, 8.1% - 444 for calcium, 4.2% - 1076 for sodium, and 2.4% - 159 for silicon respectively.

2.2.3.3 Analysis of ceramic filters by XRD

On the outer layer of the used filter, there was a layer of dark yellow residue material left on the filter surface. These products were produced by the combined interactions of mechanical and chemical loading. The former was generated by the build-up of coal ashes and particulate in the gasified stream; the chemical interaction was derived from the chemical attack to the filter matrix. This residue layer could be responsible for the reduction of filter permeability leading to a higher pressure differential across the filter. In **Figure 2.2.5**, the XRD analysis shows that the main phase composition of this outer layer are silicon oxide (SiO2), aluninum oxide (Al2O3) and silicon-alunium-silicate (Al2Si4O10). This layer was loosely adhered to the surface of the used filter, and could be easily removed from the filter surface with ultrasonic cleaning.

There was clear indication of grain growth in the outer layer and inner layer of the filter. Several small peaks observed in the spectra of the outer and the inner layer of the unused filter disappear in the spectra of the used filter. The crystal constants in the outer layer of the unused filter are 2.5901, 2.4815, 1.308, 1.3089, 1.2528, while the crystal constants in the outer layer of the used filter are 2.6192, 2.5012,1.3230, 1.3137, 1.2605 respectively. For the inner layer, the crystal constant a in the unused filter is 1.4506 while it increased to 1.4675 in the used filter. The picture of material analysis equipment is shown in **Figure 2.2.6**.

2.2.4 Conclusions of Material Laboratory Analysis

Based on the results of related investigation, the conclusions of material laboratory investigation are summarized as follows.

The unused ceramic filter is a double-layer porous candle with gray color. The broken used filter samples were in dark yellow color. The yellow color surface layer is the product of emission particle deposition and the chemical reactions between emission gases and filter material. The composition of this layer are mainly SiO2, Al2O3 and Al2Si4O10 according to the XRD analysis This layer could reduce the efficiency of ceramic filters.

The observation and analysis also indicates that there is no significant difference in morphological characteristics between used and unused ceramic filters. It seems to indicate that no obvious change in microstructure occurred after usage. But, the XRD spectrashowed that after usage the crystal structure of the main composition SiC has been changed. The crystal plan spaces

of the SiC in the outer layer were increased. For the inner layer, not only has SiC changed the crystal plane spaces, but also its grain orientation, which is different than the preferred orientation along (1034) of SiC in the inner layer of the used ceramic filter. The growing and change in microstructure of the grain caused by thermal cycle may result in great stress inside the filter. The thermal induced stresses might promote the nucleation and the propagation of micro-cracks leading to the final fatigue fracture failure of the ceramic filters.

2.3 Thermal Numerical Simulation On Back Pulse Cleaning

This thermal numerical simulation was performed on candle filters during the cold back pulse cleaning for hot gas filtration process. Based on the material laboratory investigation on used filters, it appears that there are micro-cracks developed along the inner surface of the filter. The grain deformation might be caused by a large temperature gradient along the inner surface of the filter during back pulse cleaning process. Therefore, this thermal numerical simulation is performed on a candle filter during back pulse cleaning process to gain insights into the temperature field induced therein.

2.3.1 Thermal Analysis On A Single Filter With Cold Back Pulse

A finite element analysis was initiated using the commercial finite element code ANSYS (Version 5.0). The initial analysis was focused on temperature distribution within filter during dust cake cleanup process. Half of a filter cut along the vertical plane of symmetry was used as the calculation domain.

The module was developed by dividing the computation zone into five volumes. This multizone approach was used in order to overcome the difficulties in meshing due to high slenderness ratio (length to diameter) of the filter. Discretization of the computational zone was done using two types of 3-D elements from the ANSYS element library. The bottom closed end of the filter was meshed with 3-D 10-node tetrahedral thermal solid. The rest of the cylinder was meshed with 20-node Thermal Solid Brick. In total for the entire computation domain 3598 elements were used. Connective boundary conditions were used for both outside and inside surface. The inside environmental temperature was assumed to be 40 degree C and the outside environment temperature was taken as 800 degree C, selected because it is close to the working temperature. 40 degree C at the inside was used to be close to the back pulse temperature.

The convective heat transfer coefficients were obtained using correlation for forced flow. the thermal conductivity for the filter was taken as 87-86 W/mK, a value for silicon carbide. The convective heat transfer coefficients used were 1105W/mK and 992 W/mK for inside and outside surface respectively. **Figure 2.3.1** shows a blow-up of the filter near the flange neck, (the figure also depicts the meshing of the elements) and **Figure 2.3.2** shows the temperature contour plots. The highest temperatures were on the outside surface close to the middle of the filter. The lowest temperature was on the inner surface close to the neck. The temperature variation ranges from about 567 degree C to about 405 degree C.

Based on the thermal analysis performed on a single filter during back pulse cleaning process, it appears that there is a very sharp temperature gradient existing within filter inner surface. Even though the duration of the cold pulse is very short, less than one second, but the back pulse is operating with high frequency - every twenty minutes per cycle. The repetitive thermal shock attack to filter inner surface should be the cause leading to the micro-racks within the filter inner surface.

2.3.2 Recommendation On Future Thermal Analysis

The initial analysis was done using solid wall for the filter and using steady state boundary conditions. Subsequent analysis will focus on unsteady state boundary conditions with solid wall and porous wall with unsteady state conditions. This will require coupling of heat transfer and fluid flow equations. The fluid solver that will be used is FLOTRAN which is a stand alone version of fluid flow solver in ANSYS. The analysis will include flow and pressure boundary conditions as are obtained from experiments in our laboratory.

According to the observation of the back pulse testing performed at PV A&M University, the back pulse jet was generated less than one second, and the pulse jet speed was very fast. Based on the test data, the back pulse cleaning needs a high speed jet with sufficient mass flow rate to develop an efficient dust cleaning gas stream. The jet pulse will be more efficient in cleaning as its speed increases with the pressure level of the back pulse gas, and the limit of the jet speed will be the sonic speed if there is a convergent nozzle installed in the back pulse cleaning setup. The duration of the back pulse will be limited to one second or less. Therefore, the cold back pulse jet stream shall be treated as an impulse type of loading to the hot filter.

One proposed treatment on the back pulse jet to minimize the thermal shock to the filter surface is the use of heated gas as the jet gas supply to decrease the temperature difference between the hot filter and the cold back pulse gas stream. Recently, researchers have decided that if the advanced coal powered system is to be operated less than 1,000 degree F will make the operation of the power system more feasible without sacrificing the thermal efficiency of the power system. Under this lower operating system temperature and with the use of heated back pulse gas stream will significantly reduce the chances of generating harmful micro-cracks along the inner surface of the filters during the back pulse cleaning process.

2.4 Parametric Study On Back Pulse Cleaning Mechanism

2.4.1 Introduction on particulate filtration testing campaign

Hot Particulate Removal is a critical issue for both PFBC and IGCC power systems. Filter reliability, solids loading and filter dust cake cleaning, particle morphology, chemical reactions and temperature effect are the major research topics related to hot gas cleanup. Many research institutes and researchers have devoted their efforts in upgrading filter structures and its physical and chemical properties to survive chemical, steam and high temperature attack to improve filter reliability, durability and extend filter life time. Lately, researchers have realized the importance of the understanding of back pulse cleaning mechanism to resolve issues regarding particle morphology, filter operating temperature, filter permeability variations, ash bridging and micro-thermal cracks caused by thermal shock of cold back pulse cleaning.

To evaluate the design and performance of ceramic filters and the dust cake cleaning for high temperature high pressure particulate filtration tests, different long term filter experimental campaign were conducted. To fulfill this purpose, two Advanced Particle Filter (APF) systems were complete at Tidd PFBC Demonstration Plant, in Brilliant, Ohio in late 1990 as part of the Department of Energy's (DOE) Clean Coal Technology Program. The objectives of these testing were to study the effects of particulate size distribution, cake thickness, face velocity on dust cake filtration properties, pressure and back pulse cleaning technique were studied.

But the most undesirable issues ever happened were the sudden functional and physical failures of filters prior to its designed life time. In Tidd APF filter vessel, twenty eight (28) filters failed one time. The research objectives of this paragraph are concentrated on the understanding the combined effects of pressure, filter permeability, particulate effect on dust cake, face velocity and back pulse cleaning parameters on particulate filtration process. Through the study of the fundamental parameters and their inter-actions, it would provide insights into the key factors pertinent to back pulse cleaning mechanism and the possible causes led to the failures of the demonstration testing on particulate filtration process.

2.4.2 Key parameters affecting particulate filtration process

Even though dust layer deposition on filter depends on the type of particulate, the size of the particulate, the cohesive forces between particulate itself and the filter surfaces, the chemical reaction between various of chemical elements and particulate and the temperature sintering effect, etc.; but the most important parameter to ensure the success of the particulate filtration is an efficient back pulse cleaning system.

According to the test data acquired from back pulse cleaning, a weaker starting back pulse would leave particulate residual on filter surface; and the particulate residual would make the

following back pulse cleaning less efficient even the back pulse pressure level increases. However, with the use of an efficient dust cake dislodging system, high filter permeability could be maintained for the same test environment for a long period of time. Therefore, an efficient back pulse cleaning system is indispensable throughout particulate filtration process; it would help prevent excessive dust cake deposit on filter surface to start with and also will help minimize ash bridging problems.

Based on the test data acquired in paragraph 2.1, variations of pressure field distribution can happen both outside and inside each candle filter. The change of pressure field agreed with the variations of the permeability changes of the filter measured in the bench scale filter test chamber at PV A&M University. According the test results in paragraph 2.1, we also noticed that the pressure variation is chamber pressure and filter face velocity dependent. As the mass flow rate increased through the filter chamber, the filter chamber operation pressure increased accordingly; and the pressure field fluctuation, generated by non-uniform filter permeability, could be worse with higher face velocity. More severe adverse pressure field distributions may appear in both the filter chamber and the filter cavity when filtration was performed with a higher mass flow rate. Less porous filter surface areas and dust patches would cause the reduction of filter permeability; and the lower filter permeability made it easier for the particulate to deposit on the areas already partially plugged along the filter surface. These dust cake patches accumulated on the filter surface would generate a vicious circulation to reduce the efficiency of back pulse cleaning for particulate filtration process.

Based on acquired back pulse cleaning test data, the reduction of filter permeability did make the dust dislodging less efficient even the back pulse cleaning setup remained unchanged. The reduction of back pulse cleaning efficiency enhanced the dust patch deposition on the less porous filter surface areas. With longer particulate filtration operation time, the dust patches left on the filter surface had better chance to grow and ash bridging could be developed, if sintering process is allowed in the filter vessel. The build up of dust patches could reduce the efficiency of particulate filtration and the back pulse cleaning. These deficiencies will make the filtration process difficult to control, and system failure could happen as the filtration process proceeds.

Thermal cycles, chemical attacks generated micro-cracks along the inner and outer surface wall of the filters; these micro-structural changes also led to variations of filter permeability. The various combined effects, causing the reductions of the filter permeability as soon as the particulate filtration operation started, would automatically converts the particulate filtration system into a time dependent and deficient system. This type of problem kept repeating in the field demonstration testing. The increase of the differential pressure across the filter assembly, from within the filter vessel to the plenum of the filtrated gas stream, during particulate filtration process with time is a perfect indication of the reduction of filter permeability. The deficiency of both particulate filtration and the back pulse cleaning, reported from many large scale field demonstration particulate filtration testing, confirmed that the interactions of these parameters caused particulate filtration problems. When the differential pressure across the filter assembly keeps increasing as particulate filtration process proceeds, it is a good indication that filtration

problems start to grow. As the combined effects of filter permeability reduction, less efficient dust cake dislodging, and the growth of dust residue patches work together, the filtration problem is getting worse. The vice circulation of particulate filtration process would make the particulate filtration operation more and more difficult to control as the filtration process proceeds. Therefore, the lack of an optimized dust cake dislodging system to start with, would definitely lead to an uneven dust cake dislodging distribution among filters in the filter vessel. The dust residues certainly will contribute the dust cake bridging among filters. As the filtration situation gets worse and worse, the filter vessel will be filled with uncleaned dust matrix. Finally, severe filter damages could happen or catastrophe filter failures could be generated.

2.4.3 Study on dust cake dislodging with back pulse technique

A parametric study on pulse cleaning technique was performed to address the roles of back pulse cleaning parameters. A schematic layout of the parametric testing setup is shown in **Figure 2.4.1**. The key parameters affecting back pulse cleaning efficiency include the size of the blow tube (jet lance), the relative position of the blow tube to the I.D. of the filter cavity, the fast response solenoid valve and the pressure level of the compressed air reservoir. This parametric study will help design an optimized back pulse cleaning system.

The particulate filtration testing were performed in a cold filter chamber in the laboratory of the department of mechanical engineering of PV A&M University. The interface of blow-tube with filter cavity is shown in **Figure 2.4.2**. Every different test configuration was repeated three times during the parametric study to ensure that the test data were repeatable.

2.4.3.1 Parametric study on particulate filtration process

2.4.3.1.1 Description of back pulse cleaning setup

According to METC test report of dust cake filtration (DOE/METC-91/4105), the blow-back system reservoir tank provided a volume of 2.3 cubic feet, with the pressure regulated to 225 psig from a 600 psig nitrogen source for a 6 inches I.D., 70 inches long single filter test chamber. The METC back pulse cleaning setup was equipped with a solenoid connected to the reservoir tank by 59 inches of 0.5-inch stainless steel tubing with a wall thickness of 0.035 inches. And the final connection from inside the filter vessel to a 0.375-inch tube on top of the hold down flange. At PV A&MU, the filtration chamber was fabricated with the use of a six (6) inches I.D. transparent plastic pipe. The filter chamber is equipped with a 5-foot long cavity, and a single filter was installed at the center of the chamber. The filter chamber at PV A&MU has the same configuration as that built at METC.

Back pulse cleaning design depends on the discharge of a high momentum gas jet from a pressure reservoir into the filter cavity. The momentum of the jet is transformed into a pressure increase inside the filter cavity. Based on literature research on filtration testing and the filtration

test data acquired at PV A&MU, it appeared that the energy transformation from pressure to high momentum of the cleaning jet can be acquired either with a large pipe diameter and a low pressure or with a small pipe diameter and high pulse pressure. The pulse jet generated from either design configuration was powerful enough to dislodge the dust cake deposited on filter surface. The amount of the momentum conversion within the filter cavity depends on the design configuration of the back pulse cleaning setup. Back pulse cleaning system design shall be optimized to ensure the success of filtration process.

Because flour is clean, dry, not sensitive to moisture and light weight; it is easy to be cleaned and filled and retrieved into and out of the filtration chamber. Flour cake and its residual patches could be easily recognized through the transparent filtration chamber. Due to its light weight, flour reentrainment flow could be observed during the filtration process. Therefore, flour was selected as the first particulate candidate for filtration testing.

2.4.3.1.2 Study on compressed gas reservoir and size of blow-tube I.D.

To study the interaction between the reservoir pressure and the I.D. of the blow-tube, the back pulse cleaning setup was configured with a variety of combination between different pressure ranges of back pulse pressure reservoir, the I.D. of the blow tube. After a proper combination of pressure reservoir and blow-tube size is selected, the effect of the position of the blow tube relative to filter cavity was investigated. The pressure level of the gas reservoir ranged from hundreds of psig to 15 psig. The I.D. of the blow-tube ranged from 3/8, 1/2, 3/4, 1.0 to 1.5 inches.

In the parametric study, a 1.2-cubic foot gas reservoir was designed for the pulse cleaning testing. This gas mass needed to be fed into the filter chamber instaneously with the use of a fast response normally closed solenoid valve, with a response time of 700 milli-seconds or less, to provide the high mass flow rate as required for dust cake dislodging work.

A six inches thick flour bed was installed on top of the bottom sealing plug within the filtration chamber prior to the injection of nitrogen or compressed air into the filtration chamber through the gas inlet port at the bottom sealing plug of the filtration chamber. A very heavy dust loading was generated through the flour bed as the gas stream flew through it. Light weighted dry flour particulate was easily blown up to fill the entire filtration chamber. A 5 millimeter thick flour cake was deposited on the external surface of the filter within a-five-minute time period with a mass flow rate of 2 SCFM. This type of particulate loading was significantly heavier than those experienced in the field testing, typically a 5,000 ppmw concentration loading.

Flour cake could be easily dislodged by back pulse cleaning technique with a pulse jet stream released from a 15-psig pressure reservoir (1.2 cubic feet tank volume) through a 1.5 inches I.D. pulse plenum. The low pressure, large I.D. pulse plenum setup generated sufficient momentum for the pulse jet to clean the flour cake. This type of low pressure, large plenum I.D. setup design was

proved to be an efficient pulse cleaning configuration for dust cake cleaning performed on various materials, including coal ash, flour/coal ash, flour/iron-oxide, and coal ash/iron oxide mixtures.

To perform the pulse cleaning study economically, a large pulse stream plenum and a large I.D. blow-tube combination was selected to use a lower pressure gas reservoir. To further minimize the frictional loss for the gas stream, only one normally closed solenoid valve was installed between the gas reservoir and the blow-tube.

According to pulse testing, it appeared that the pressure level of the pulse pressure reservoir needs to be increased sharply as the I.D. of the blow tube decreased to perform an efficient dust cake dislodging task. The frictional loss of gas jet stream experienced as it traveled along the back pulse plenum, jet pressure losses through various area changes along the pulse plenum system, its valves and the energy loss due to the reduction of blow-tube cross section area were responsible for the requirement of a high pressure of gas reservoir.

To further differentiate the effect of the frictional loss, the plenum design and the blow-tube I.D., the back pulse cleaning system was adjusted to investigate each parameter. To minimize the frictional loss for jet stream along the plenum, the length of gas stream conduct was adjusted to bring the gas reservoir as close to the filter chamber as possible. To reduce the pressure loss through different valves and the size changes of plenum tubing size, one size of plenum was utilized for back pulse cleaning. To study the effect of blow-tube I.D., only one tube I.D. was used for each testing.

After post data analysis, it appeared that the blow-tube I.D. and the size of gas stream plenum dominated the pressure loss for back pulse cleaning process. Theoretically, it is evident that as the cross section area of the blow tubing reduces, higher jet velocity will be needed to provide a fixed amount of gas flow rate to compensate the area reduction compared to a larger I.D. system design. For circular tubing, the cross section area is square related to the I.D. of the tubing. The reduction of tubing size automatically increased the jet stream velocity, but the sonic velocity will be the limit for a convergent type flow system.

As reflected by the pulse system setup of a large pressure reservoir and a small I.D., the incraesed jet stream velocity needs to be match the fixed volume of gas stream supply for dust dislodging. However, as the I.D. of the blow-tube is reduced to a certain range and the jet stream speed is limited to sonic velocity, extra energy loss would be induced in the gas stream flow. This type of energy loss had been confirmed with the use of either small size blow-tube or an extra long length of gas stream plenum connected to the blow-tube. Loud noise were audible as the energy loss happened during the filtration processes. Severe residual dust patches left on the uncleaned filter were repeatable found as the back pulse jet energy declined during the filtration process. The failure of dust lodging was caused by a dynamic choke, experienced when the blow-tube I.D. was reduced beyond the limit, no matter how high the back pressure of the gas reservoir could be. This reasoning was confirmed by additional testing on the cleaning of the residual dust patches left on the uncleaned filter. As soon as the energy loss constraints were removed, the

residual dust patches could be thoroughly cleaned. The healthy back pulse cleaning setup could perform successful dust dislodging task repeatly with ease.

Based on the test results, it was then concluded that 1) back pulse cleaning is an efficient technique for dust cake dislodging application, 2) the gas stream plenum design shall be free of energy loss constraints, 3) with the use of a low pressure gas reservoir, the reduction of tubing I.D. significantly affect the mass flow rate required for a successful dust dislodging and 4) the test configuration of the use of a large diameter gas stream plenum and a large I.D. blow-tube with a low pressure gas reservoir would be the most economical one to complete the parametric testing.

Therefor, the selected back pulse cleaning configuration for the rest of filtration testing at PV A&M University was the combination of a low pressure gas reservoir and large I.D. blow-tube.

2.4.3.1.3 Study on the relative position of blow-tube to the filter cavity

To understand the effect of the relative position of the blow-tube to the filter cavity, a fixed back pulse cleaning setup was used to perform dust cake dislodging testing. The blow-tube was adjusted in axial and lateral direction relative to the filter cavity.

For axial position testing, the blow-tube was positioned 2.0, 4.0 and 6.0 inches above the filter cavity, and also inserted 3.0, 6.0 and 9.0 inches within the filter cavity prior to the back pulse jet stream was released into filter cavity after a thick layer of dust cake was deposited on filter surface. Based on the test results, it appeared that the effect of the relative axial position of the blow tube was not significant for dust cake dislodging when the blow-tube was located at those preset axial locations as long as the back pulse cleaning setup is strong enough to clean the dust cake when the blow-tube was 2.0 inches above the filter cavity. It is very interesting to find out that as the blow-tube was inserted into the filter cavity, pressurized jet stream was able to clean the dust cake located at areas close to filter flange. These test data indicated that the pulse jet stream self-adjusted itself very quickly as it entered the filter cavity. As long as the jet stream is positioned along the axis of the filter cavity, the relative axial position of the blow-tube is not a significant parameter for dust cake dislodging.

For lateral shift of the blow-tube relative to filter axis was performed with the use of a special jet inlet adapter. This study was performed with the same test setup for the axial position testing except that the axis of the blow-tube was adjusted at 1/4 and 1/2 of the radius of filter cavity. A extreme case was studied by injecting the gas stream into filter cavity about 3.0 inches above the filter cavity, but the jet stream was injected perpendicular to filter cavity axis. Uneven dust dislodging was observed as the jet stream deviated from filter cavity axis. The horizontal inlet jet lost more energy in the three different jet inlet position.

It was concluded that the pulse jet stream should be positioned along the filter cavity axis and the effect of the aixal position of the pulse stream is not significant for dust cake dislodging process.

2.4.3.1.4 Study on particulate effect during filtration process

To evaluate the filtration performance of candle filter, the differential pressure values (Delta P) across the cleaned filter and the filter with dust cake buildup were measured throughout the filtration process. The Delta P value measured from a cleaned filter is the total resistance induced by a clean filter and the filtrated flow plenum system. The Delta P difference measured between a dust cake coated filter and a clean filter is the gas flow resistance of the dust cake. Through the measurement of Delta P throughout the filtration testing, the performance of the filtration system can be characterized.

To gain insights of particulate effect on filtration process, different particulate materials were evaluated in this study. Observation of dust reentrainment and measurement of dust cake thickness were also conducted in the transparent cold flow filtration chamber. Besides the study on single phase material, mixtures of different type of particulate were also evaluated during filtration testing to understand the effect of particulate mixing on filtration permeability and the reentrainment flow.

Dust cake made of flour, waste iron oxide and coal ash, originating from the Curtis-Wright PFBC facility, were evaluated first. Flour is a light weight material, with a specific gravity of about 0.5. The specific gravity of coal ash and iron oxide is approximate 1.0 and 0.9. The characteristics of the dust candidate relies on its physical properties and the filtration environment.

Flour is dry and very easy to work with and its dust cake can be removed with least gas reservoir pressure. Coal ash is also not sensitive to moisture, which makes it easy to load and retrieve from the filter chamber for filtration testing. Even though coal ash is the heaviest one, a high density coal ash mixed gas flow can be generated with a dry gas flow of 2.0 scfm flow rate. Higher mass flow rate, 6.0 scfm, was strong enough to agitate the coal ash every where in the 6.0-inch I.D. filter chamber. Coal ash dust cake can be cleaned by back pulse cleaning without difficulty. However, iron oxide is the most difficult material to work with. The key issue of handling iron oxide is due to the agglomeration of iron oxide into large cluster of materials. Iron oxide also has a strong affinity to moisture, which made it very difficult to feed or retrieve form the filtration chamber during filtration testing. Wet iron oxide has a very strong adhesion force toward the materials it contacted. This special characteristic made iron oxide dust cake very difficult to clean completely away from filter surface. To avoid the unexpected moisture effect during the filtration study, every particulate candidate was dried prior to the filtration testing was performed.

After the particulate candidate was characterized, mixture of flour and iron oxide and mixture of coal ash and iron oxide were utilized to buildup different dust cakes on candle filter. With the use of the same back pulse cleaning setup, every dust cake had been successfully removed from IF&P ceramic filter. After drying the particulate, dust cake dislodging task was easier than working with wet particulate. The measured Delta P values through different dust cakes indicated

that the adding of foreign materials to coal ash would not cause higher Delta P value during the filtration process.

Test data also indicated that a specific threshold pulse pressure is required to clean the dust cake. Pulse pressure slightly above the threshold pressure is strong enough to clean the dust cake. Excess dust loading would create residual dust layer, which increases Delta P through the dust cake. Thicker dust cake needs stronger back pulse pressure for dust cake cleaning. However, the use of a stronger pulse pressure can clean filter surface efficiently such that the ensuing excess dust loading can be better cleaned than the use of a weak cleaning pulse pressure as the filtration process started.

2.4.3.1.5 Study on the leakage of back pulse cleaning system

To investigate the issue of the leakage of the back pulse system, two different testing were performed. One was the releasing of the pressure of back pulse gas reservoir, and the other was the plenum cracking during back pulse cleaning process.

The sealing o-rings on top of the gas reservoir were removed from the top chamber sealing adapter as simulation of gas reservoir leakage for dust cake dislodging testing. The leakage of gas reservoir lowered the pressure level of the reservoir instaneously. The operation of a large air compressor could not keep reservoir tank pressure at preset back pulse tank pressure. The reduced reservoir tank pressure affected the efficiency of the back pulse cleaning. Although the mechanical clearance between the sealing surfaces is less than 0.001 inches only, the gas reservoir pressure reduced very quickly. Even though a large air compressor was operating to deliver a 6-scfm air flow to the gas reservoir, the reservoir pressure could not exceed 10 psig. The back pulse cleaning efficiency was badly reduced with this type of leakage configuration. A larger leakage through the back pulse cleaning system could reduce gas reservoir pressure even more to disable the back pulse cleaning system.

A 1/4-inch ball valve, installed on the O.D. of the filter sealing adapter, was left open prior to the back pulse jet stream was injected into its plenum. The leaking of the plenum close to the entrance to filter cavity significantly affect the cleaning efficiency of the back pulse cleaning effect. Heavy residual dust patches were spread all over the filter surface.

These simulation of the leakage of the back pulse system revealed that the entire filtration system shall be leak free to ensure the success of dust cake dislodging operation. If the candle filter cracked or fractured during the filtration process, these leakage would make the entire filtration system less efficient.

As soon as leakage developed within the filtration system either from the back pulse cleaning system or the fracture of candle filter, the leaked filtration system would inevitably invited more dust patches on filters in the filtration chamber. The extra deposition of dust cakes on filters automatically increases the Delta P value which will make the back pulse operation more difficult.

The vicious circulation of the dust dislodging operation would eventually paralyze the filtration system. As the reduction of dust cake dislodging efficiency get worse along with the proceeding of the filtration process, the filter chamber would be filled with more uncleaned dust. The poor operation of the filtration process would eventually cause the failure of the entire filtration system.

2.4.3.1.6 Study on filter permeability variation effect on dust cake dislodging

To understand the effect of filter permeability variations on dust cake dislodging, the used IF&P filter was utilized for flour filtration and flour cake dislodging. Filter permeability variations of the used filter was characterized before with clean nitrogen. The permeability variations were found distributed along filter axial and circumferential directions. This study is served to gain insights into the effect of filter permeability effect on subsequent filtration and dust dislodging process.

A 6-inch flour bed was filled within the filtration chamber, and a 6-scfm air flow rate was used to build the flour cake on the filter surface. Due to the light weight of the flour, the flour dust was filled everywhere within the filtration chamber. Because the high air flow rate, the flour cake deposited on the filter surface was not uniformly deposited. Different size of slots, possibly caused by the non-uniform air flow, were observed on flour cake.

After back pulse cleaning, minor flour residual patches were found left on the used filter surface. The bottom section of the filter surface (section 4 of permeability test setup) was best cleaned with the pulse cleaning, which agreed with the permeability distribution of this used filter. Flour patches were more densely distributed in section 2 and section 3 areas of the used filter. In the less permeable filter areas, large size of flour patches were visible, and the flour patches were also thicker than those in section 4. Similar result was also found along the circumferential direction of the used filter.

The pattern of the flour cake patch distribution on the used filter is consistent with the variations of filter permeability characterized in section 2.1, more and thicker flour patches were found in the less permeable filter section areas. Filter permeability variations along filter surface would cause uneven dust dislodging even the back pulse cleaning setup remained unchanged.

The finding of filter permeability effect on dust cake dislodging shed light on the importance of preventing permeability variations from being developed on filter surface during filtration process. Based on test data of iron oxide, it was shown that if the filtrated particulate has a strong affinity to filter surface, filter surface could be plugged with fine particulate. The plugging on filter surface would cause filter permeability variations.

This study was performed at room ambient environment, therefore, thermal chemical effect on the interaction between filter surface and dust patches needs be further investigated.

2.5 Failure Analysis On Ceramic Candle Filter

This section is devoted to the failure analysis of the candle ceramic filter utilized for the filtration process study. The possible causes of filter failures include mechanical loading applied on filters, thermal shock during back pulse cleaning, thermal upset on filters by system shut-down and re-start operation, thermal chemical reaction between filter and coal ash and back pulse cleaning efficiency. The process of elimination will be utilized for the failure analysis described herein.

2.5.1 Study on impact of mechanical load on candle filter

To investigate the mechanical integrity of subject candle filters, different mechanical loading were performed on used and unused filters. The mechanical loading includes (1) hundreds cycle of back pulse jet loading testing, (2) acceleration testing, (3) impact testing and (4) long term static loading testing. For each kind of the mechanical testing, the filter was fixed at the filter flange. These mechanical loading were more severe than those experienced in the filter chamber during the filtration testing. This testing is designed to investigate individual mechanical loading effect on filter integrity.

(1) Hundreds of back pulse jet were injected to candle filter throughout the filtration study. The candle filter was pulse so hard that post pulsed filter vibration was observed after each back pulse cleaning for the used and unused filters. The total number of pulse induced vibration was estimated more than three hundred times. The filters were not physically damaged throughout the back pulsed jet loading.

(2) The strength of acceleration testing loading applied on filters was approximate a 1.5-g level of acceleration, intermittently applied on filters for about 2 seconds for each loading. Twenty acceleration loadings were applied on the used and unused filters. No physical damage was detected after the acceleration testing.

(3) The impact loading on the filter was applied to let the filter chamber free fall from the vertical position to the horizontal position on carpeted floor. The impact g level was very high, and this kind of testing was applied twice on used and unused filters. No physical damage was detected after the impact testing.

(4) Long term static loading testing was applied to tested filters with the filter installed in the filter chamber and the filter chamber was laid horizontally on the floor. The weight of the filter developed 1.25 Kg-Meter (9.02 lb-ft) torque on the filter neck at filter flange area. This static loading test was performed for two weeks for used and unused filters. No physical damage was detected after the static loading test.

Based on the test results of the mechanical loading testing, the filter was robot enough to survive individual mechanical loading. The field tested filters should be able to survive filtration mechanical loading such as the form drag and flow induced vibration in the filter chamber as long as the filter physical strength were not severely degraded by the filtration environment.

2.5.2 Study on thermal shock on candle filter during back pulse cleaning

Based on the thermal analysis performed on a single filter during back pulse cleaning process in paragraph 2.3, it appears that there is a very sharp temperature gradient existing within filter inner surface. Even though the duration of the cold pulse is very short, less than one second, but the back pulse is operating with high frequency - every twenty minutes per cycle. The repetitive thermal shock attack to filter inner surface should be the cause leading to the micro-racks within the filter inner surface.

Based on the observation and analysis performed in material laboratory analysis, it was shown that there is no significant difference in morphological characteristics between used and unused ceramic filters. The test results seem to indicate that no obvious change in microstructure occurred after usage. But, the XRD spectrashowed that after usage the crystal structure of the main composition SiC has been changed. The crystal plan spaces of the SiC in the outer layer were increased. For the inner layer, not only has SiC changed the crystal plane spaces, but also its grain orientation, which is different than the preferred orientation along (1034) of SiC in the inner layer of the used ceramic filter. The growing and change in microstructure of the grain caused by thermal cycle may result in great stress inside the filter. The thermal induced stresses might promote the nucleation and the propagation of micro-cracks leading to the final fatigue fracture failure of the ceramic filters.

Based on the testing of the effect of filter permeability on dust cake dislodging, filter permeability variations along filter surface did affect the efficient of dust cake dislodging. The less porous filter surface areas are prone to buildup dust cake patches. The growth of dust cake patches would make the filtration and dust cake dislodging more difficult to carry on. Therefore, it is critical to prevent permeability variations from being developed on filter surface during filtration process. The strong affinity of filtrated particulate to filter surface could cause the plugging of filter surface with thermal reacted products. The longer the dust cake patch left on filter surface, the worse the sintering of the dust patch would be on filter surface. These patch plugging on filter surface would cause filter permeability variations, leading to reduction of filtration and dust dislodging efficiency.

Thermal shock induced by cold gas back pulse for dust cake cleaning caused the development of micro-cracks along inner filter surface. These cracks might be responsible for the variations of filter permeability variations experienced by used filters. The micro-cracks might be the precursors for the development of residual dust patch. Therefore, the back pulse jet stream should be pre-

heated to minimize the temperature gradient generated along filter inner surface for each back pulse cleaning cycle.

2.5.3 Study on thermal upset on filters during system shut-down and re-start

The field tested filtration system had been through several system shut-down and re-start cycles. Through each cycle, the filtration system would experienced thermal upset. Based on the current filtration study, physical damages on ceramic filters caused thermal upset should be limited. However, the long period of time experienced through system cooling and re-heating might generate issues related to moisture condensation.

Many research institutes found that the filter physical properties had been degraded at high operating temperature (typical at 800 degree C), including the reduction of mechanical tensile strength and filter toughness. However, the cooling of filtration system within a long period of time did not seem possible to create further material degradation, because most filter physical properties could be recovered as the ambient temperature dropped to room ambient temperature.

As the filtration system returned to room ambient temperature, water content of steam would be condensate back to liquid state. Once the filtration system was open-up, more moisture could be introduced into the filtration system. These moisture could be absorbed by coal ash and dust cake patches left in the filter vessel and on the filter surfaces. As pointed out in the parametric study on particulate filtration process, once the coal ash and the dust cake patches got wet, these ash related products had a strong affinity to filter surfaces and the internal surface of the filter vessel. These strong adhesion between coal ash products to filter surfaces and filter vessel surface would provide an excellent environment for ash bridging, if the coal ash and dust cake patches could not be removed form those surfaces successfully.

The plugging of the filter surfaces, even though small percentage to start with, could be accelerated as the filtration and dust cake removal efficiency declined. The kept increased Delta P could be a good indication of the plugging phenomena explained.

Therefore, the damages caused by system shut-down should be derived from the wet coal ash products and dust cake left in the filtration system, causing more difficulty for dust cake removal after the filtration system resumed the filtration operation conditions.

2.5.4 Study on thermal chemical reactions of coal ash on filters

It was speculated that thermal chemical reactions between coal ash and filter surface might be the cause of the growing of dust cake patches and the finding of ash bridging. Researches on thermal chemical reaction were performed by few research institutes, but there was no direct clue proving that the chemical ingredients were responsible for the buildup of dust cake patches on

filter surface. METC and STC/Westinghouse had performed series testing to investigate the thermal chemical attack of chemical ingredients to ceramic filters.

This research work was concentrated at cold flow study on filtration process, high temperature chemical reaction study is beyond the scope of the investigation work. However, if the dust cake patches could not be removed from filter surface, long term of thermal exposure of these dust patches under compressive flow pressure during the filtration process might provide a sintering environment for the growth of dust cake and ash bridging.

2.5.5 Study on back pulse cleaning effect on filters

Based on the study performed back pulse cleaning, the test data indicated that a specific threshold pulse pressure is required to clean the dust cake. Pulse pressure stronger than the threshold pressure is required to clean the dust cake. Excess dust loading could generate residual dust layer, which caused Delta P value increased through the dust cake. Thicker dust cake needs stronger back pulse pressure to have the dust cake cleaned. Stronger pulse pressure is always recommended to clean filter surfaces to ensure the success of dust cake dislodging can be maintained through the filtration process.

However, if pressure leakage was developed within back pulse cleaning system, dust cake dislodging efficiency reduced significantly. The reduction of dust cake dislodging could be most critical issue leading to the failure of filters. As the dust cake dislodging efficiency declines, more and more uncleaned dust or ash bridging could be left within the filtration chamber. At high operation temperature, thermal induced strain for mismatched thermal expansion coefficient would develop a large thermal plastic deformation on filters.

The micro-cracks on filter surface or unexpected shear forces induced by thermal mismatch of coal ash and filters for a shut-down filtration system might generate a very large bending moment applied on filters. These large deformation of filters and large thermal induced stress could cause the failures of ceramic candle filters.

According to the analysis of the possible causes led to the failures of the candle filters, it is concluded that the failure of ceramic candle filters should be the combined interactions of various factors described herein. High temperature gradient of back pulse cleaning, thermal chemical reaction of coal ash products with filter surface, thermal upset of the filtration system via system shut-down and re-start, and the reduction of dust cake dislodging efficiency are the possible causes for the failures of ceramic candle filters.

3.0 CONCLUSION

This research work was concentrated on a cold flow study on filter characterization, a material laboratory analysis on used and unused filters, a numerical thermal analysis on cold back pulse cleaning process and a parametric study on particulate filtration process. Based on the test results of the tests performed at PV A&MU, a failure analysis was then performed. According the process of elimination, it was concluded that the causes of the failures of filters during field demonstration testing should be a multi-cause interactions between coal ash, filter surfaces and the system operation. To improve the filter operation process and prevent the failure of filters from happening, the recommendations are summarized below.

The conclusions of the subject research work and recommendations for future research work to provide a better filtration operation are listed as follows:

(1) The back pulse gas stream needs be pre-heated to reduce the temperature gradient developed during the back pulse cleaning cycle.

(2) A strong back pulse gas stream shall be applied to filters during dust cake dislodging process.

(3) The size of the back pulse blow-tube should be kept as large as possible to ensure an efficient back pulse cleaning setup.

(4) Back pulse cleaning system shall be maintained leakage free to ensure the success of long term back pulse cleaning.

(5) Filter physical strength shall be improved to eliminate the chance causing premature filter failure due to low thermal strength or low thermal toughness.

(6) Moisture condensation shall be eliminated from the filtration system during system shut-down process.

(7) More research work needs performed on high temperature chemical reactions of coal ash products on ceramic filters.

(8) More study on long term dust cake sintering development.

(9) Use particulate additive as required to make particulate flow and dust cake dislodging easier to facilitate filtration and dust cake dislodging work.

(10) Use proper chemical sorbents to remove chemical ingredients that cause dust cake sintering problem prior to the filtration operation.

References

Alvin, M.A., Tressler, R.E., Lippert, T.E., Diaz, E.S. and Smeltzer, E.E., 1994, "Durability of ceramic filter" Proceedings of the Coal Fired Power System 93 - Adavances in IGCC and PFBC Review Meeting, U.S. Department of Energy

Bruck, G.J. and Isaksson Juhani, 1994, "Karhula Hot Gas Cleanup Test Results" Proceedings of the Coal Fired Power System 93 - Advances in IGCC and PFBC Review Meeting, U.S. Department of Energy

Goldsmith, R.L., September, 1992, "Ceramic Filters for Removal of Particulate from Hot Gas Streams", Proceedings of the Twelfth Annual Gasification and Gas Stream Systems Contractors Review Meeting, Volume 1

Heather M. McDaniel, Ronald K Staubly, Venkat K. Venkataraman, June, 1994, "Proceedings of the Coal Fired Power System 94 - Advances in IGCC and PFBC Review Meeting" Volume 1, U.S. Department of Energy

Smoot, L.D. and Smith, P.J., 1985, "Coal Combustion and Gasification" Plenum Press, New York, NY

Klignspor, J.C. and Cope, D., FGD Handbook, May, 1987, "Flue Gas Desulfurization Systems" ICEAS/B5, International Energy Agency Coal Research, London, United Kingdom

Mei, D., 1995, "Characterization and Testing of Ceramic Filter and Dust Cake for Hot Gas Cleanup Program", Summer Research Study report presented at METC, United States Department of Energy

Pontitus, D.H. and Starrett, H.S., 1994 "Properties of Ceramic Candle Filters" Proceedings of the Coal Fired Power Systems 93 - Advances in IGCC and PFBC Review Meeting, U.S. Department of Energy

Zievers, J.F., Eggerstedt, P.M., Aguilar, P.C. and Zievers, E.C., 1993, "Some Ceramic Options" Proceedings of the Coal Fired Power Systems 93 - Advances in IGCC and PFBC Review Meeting, U.S. Department of Energy

Khan, R., Huque, Z., Mei, D., 1997, "Preliminary and Pressure Field Study On New and Used Ceramic Candle Filters" Engineering & Architecture Symposium Proceedings - PV A&M University

R. Clift and J.P.K. Seville, "Regeneration Of Rigid Ceramic Filters" Gas Cleaning At High Temperatures

APPENDIX A

PERMEABILITY TEST DATA OF UNUSED AND USED FILTERS

UNUSED FILTER

SECTION 1 EXPOSED SECTION 2 EXPOSED SECTION 3 EXPOSED SECTION 4 EXPOSED

Time(min)	Press(psi)	Time(min)	Press(psi)	Time(min)	Press(psi)	Time(min)	Press(psi)
0.00	10.72	0.00	10.79	0.00	10.65	0.00	10.37
0.50	5.08	0.50	5.12	0.50	5.01	0.50	4.96
1.00	2.43	1.00	2.48	1.00	2.37	1.00	2.35
1.50	0.69	1.50	0.75	1.50	0.70	1.50	0.63
1.68	0.00	1.75	0.00	1.71	0.00	1.69	0.00

SECTION 1 EXPOSED SECTION 2 EXPOSED SECTION 3 EXPOSED SECTION 4 EXPOSED

Time(min)	Press(psi)	Time(min)	Press(psi)	Time(min)	Press(psi)	Time(min)	Press(psi)
0.00	15.40	0.00	15.13	0.00	15.34	0.00	15.63
0.50	10.85	0.50	10.59	0.50	10.88	0.50	10.92
1.00	4.95	1.00	4.78	1.00	485	1.00	5.02
1.50	2.10	1.50	2.15	1.50	1.98	1.50	2.05
2.00	0.48	2.00	0.33	2.00	0.36	2.00	0.44
2.11	0.00	2.08	0.00	2.10	0.00	2.18	0.00

UNUSED FILTER

SECTION 1 EXPOSED		SECTION 2 EXPOSED		SECTION 3 EXPOSED		SECTION 4 EXPOSED	
Time(min)	**Press(psi)**	**Time(min)**	**Press(psi)**	**Time(min)**	**Press(psi)**	**Time(min)**	**Press(psi)**
0.00	**20.27**	**0.00**	**20.39**	**0.00**	**20.22**	**0.00**	**20.37**
0.50	**16.14**	**0.50**	**16.09**	**0.50**	**16.17**	**0.50**	**16.10**
1.00	**11.29**	**1.00**	**11.33**	**1.00**	**11.23**	**1.00**	**11.29**
1.50	**6.59**	**1.50**	**6.61**	**1.50**	**6.58**	**1.50**	**6.77**
2.00	**2.98**	**2.00**	**2.93**	**2.00**	**2.88**	**2.00**	**3.02**
2.50	**0.82**	**2.50**	**0.84**	**2.50**	**0.78**	**2.50**	**0.85**
2.72	**0.00**	**2.75**	**0.00**	**2.68**	**0.00**	**2.70**	**0.00**

USED FILTER

SECTION 1 EXPOSED		SECTION 2 EXPOSED		SECTION 3 EXPOSED		SECTION 4 EXPOSED	
Time(min)	Press(psi)	Time(min)	Press(psi)	Time(min)	Press(psi)	Time(min)	Press(psi)
0.00	10.79	0.00	10.75	0.00	10.75	0.00	10.63
0.50	7.57	0.50	5.98	0.50	4.55	0.50	8.44
1.00	5.66	1.00	2.94	1.00	2.89	1.00	7.31
1.50	4.08	1.50	1.83	1.50	1.53	1.50	6.05
2.00	2.84	2.00	0.29	1.85	0.00	2.00	4.78
2.50	0.87	2.13	0.00			2.50	3.28
2.86	0.00					3.00	1.11
						3.50	0.12
						3.70	0.00

SECTION 1 EXPOSED		SECTION 2 EXPOSED		SECTION 3 EXPOSED		SECTION 4 EXPOSED	
Time(min)	Press(psi)	Time(min)	Press(psi)	Time(min)	Press(psi)	Time(min)	Press(psi)
0.00	15.86	0.00	15.38	0.00	15.82	0.00	15.80
0.50	10.66	0.50	12.82	0.50	12.23	0.50	12.13
1.00	6.85	1.00	7.81	1.00	7.37	1.00	9.14
1.50	3.72	1.50	4.37	1.50	3.01	1.50	6.58
2.00	1.62	2.00	1.86	2.00	0.87	2.00	4.49
2.50	0.41	2.50	0.49	2.40	0.00	2.50	2.78
3.00	0.00	2.61	0.00			3.00	1.48
						3.50	0.60
						4.00	0.12
						4.25	0.00

USED FILTER

SECTION 1 EXPOSED		SECTION 2 EXPOSED		SECTION 3 EXPOSED		SECTION 4 EXPOSED	
Time(min)	**Press(psi)**	**Time(min)**	**Press(psi)**	**Time(min)**	**Press(psi)**	**Time(min)**	**Press(psi)**
0.00	**20.57**	**0.00**	**20.15**	**0.00**	**20.60**	**0.00**	**20.42**
0.50	**15.16**	**0.50**	**14.78**	**0.50**	**13.64**	**0.50**	**18.01**
1.00	**12.75**	**1.00**	**10.64**	**1.00**	**9.04**	**1.00**	**16.19**
1.50	**8.17**	**1.50**	**7.01**	**1.50**	**3.96**	**1.50**	**14.64**
2.00	**5.27**	**2.00**	**4.03**	**2.00**	**1.88**	**2.00**	**13.03**
2.50	**2.61**	**2.50**	**1.22**	**2.50**	**0.35**	**2.50**	**11.06**
3.00	**1.02**	**3.00**	**0.25**	**2.79**	**0.00**	**3.00**	**9.92**
3.50	**0.00**	**3.09**	**0.00**			**3.50**	**7.04**
						4.00	**4.55**
						4.50	**2.07**
						5.00	**0.31**
						5.12	**0.00**

IGCC R&D Issues

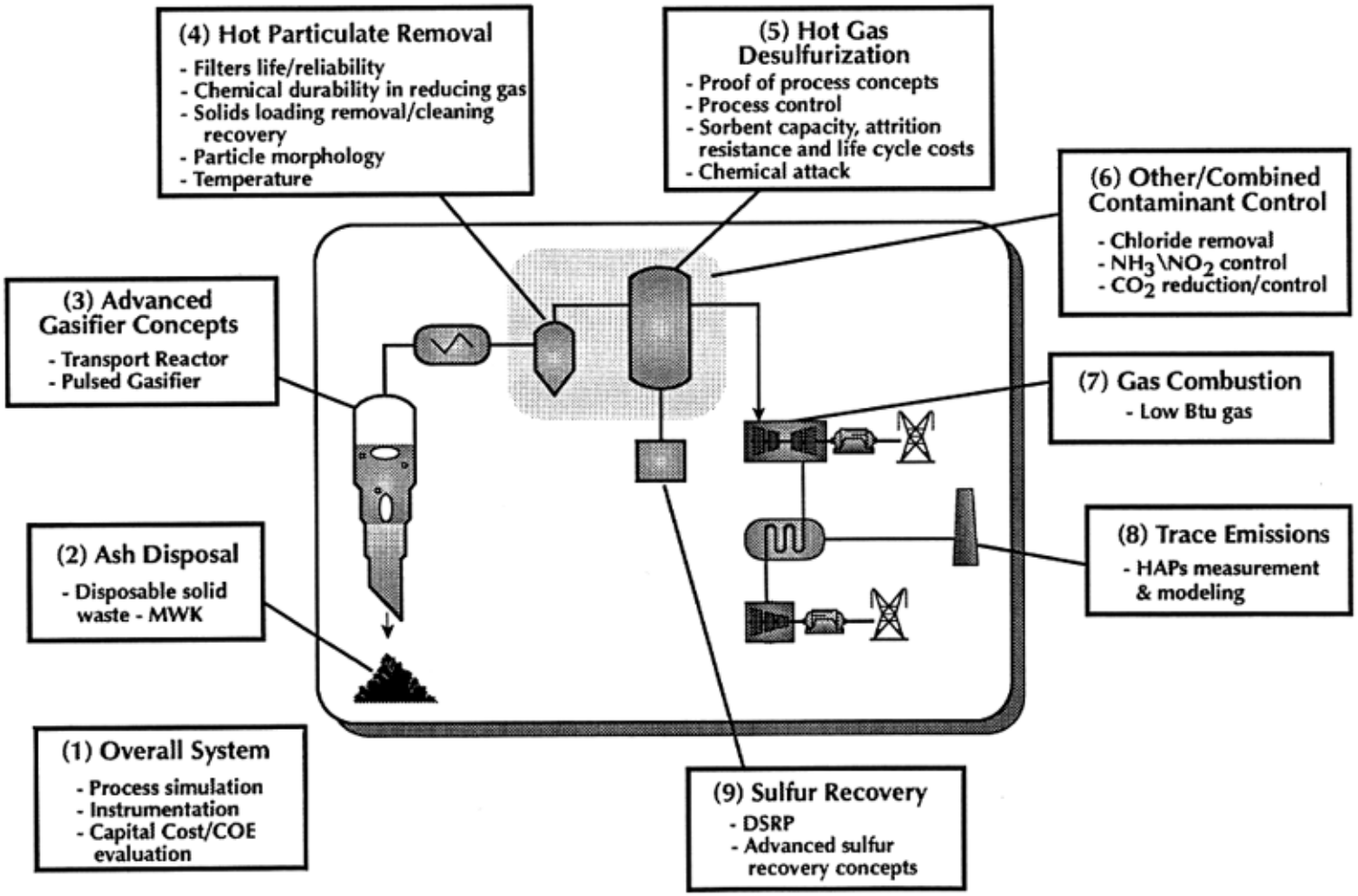

Figure 1-1 Schematic of IGCC and R&D Issues

PFBC R&D Issues

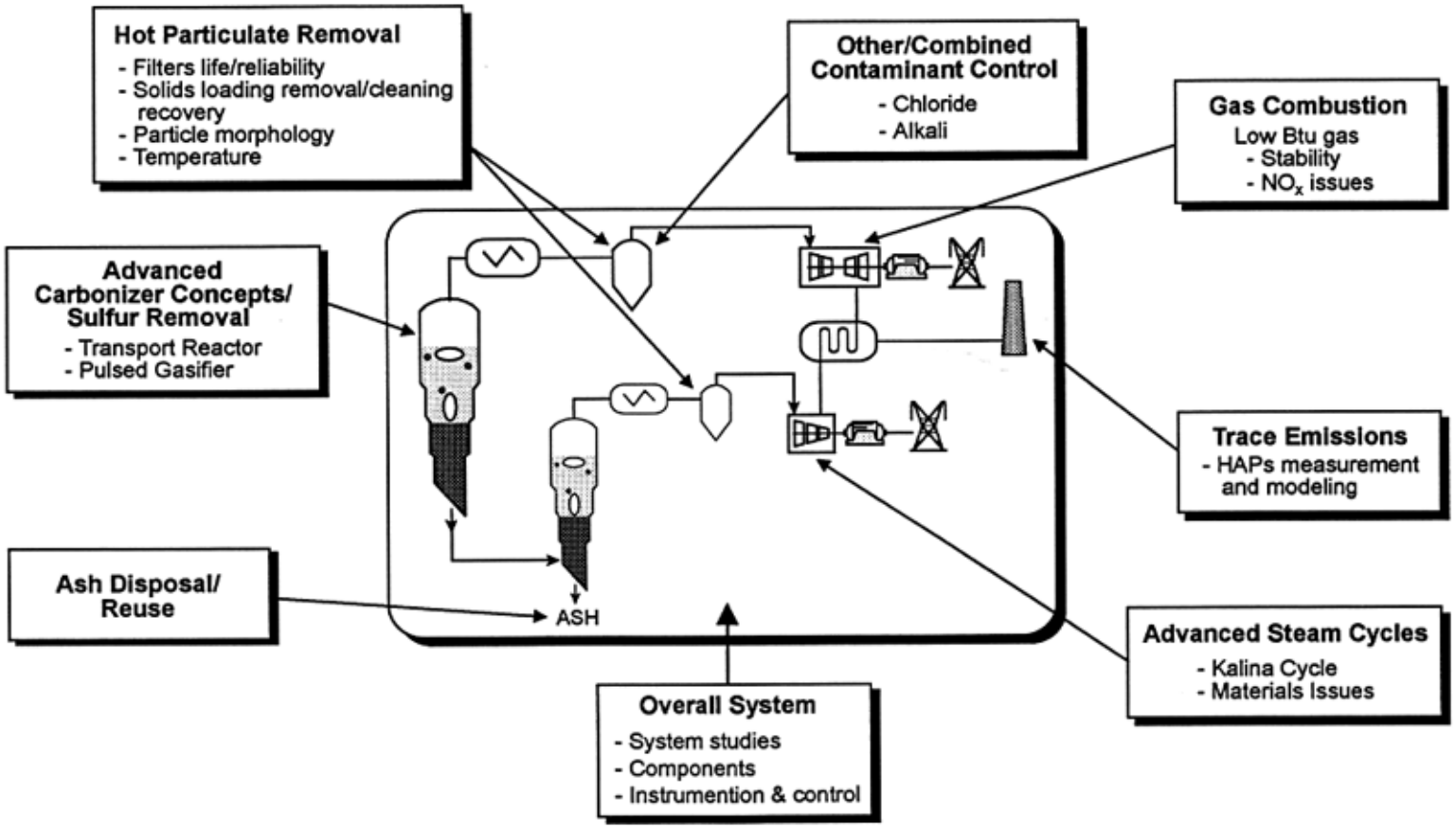

Figure 1-2 Schematic of PFBC and R&D Issues

AEP Candle Failure Locations

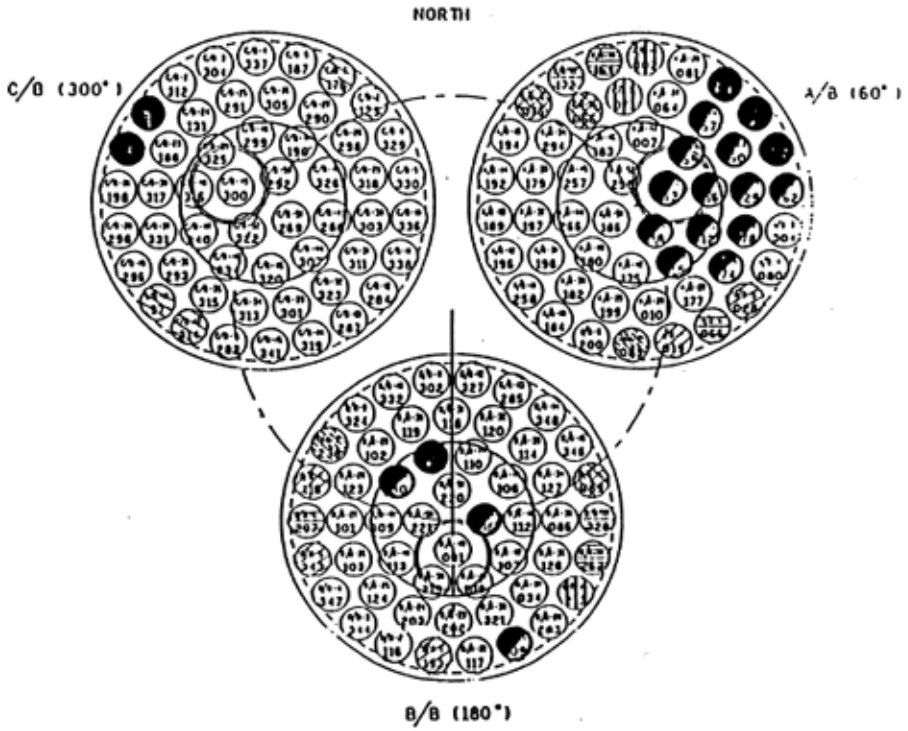

December 1992

Figure1-3 AEP candle filter failure locations

MAA
07-28-93

Westinghouse
Science & Technology Center

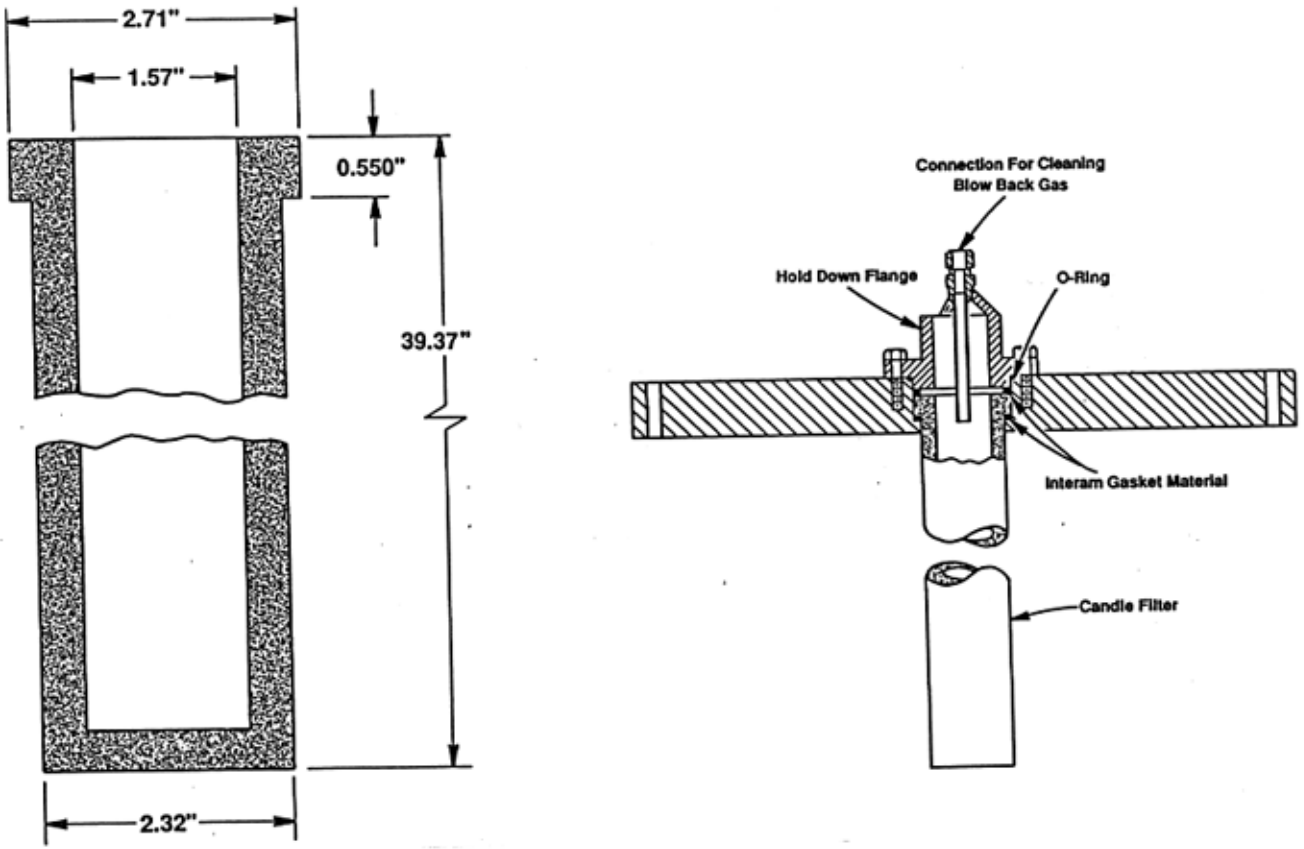

Figure 2-1-1 Schematic of candle filter and top sealing configuration

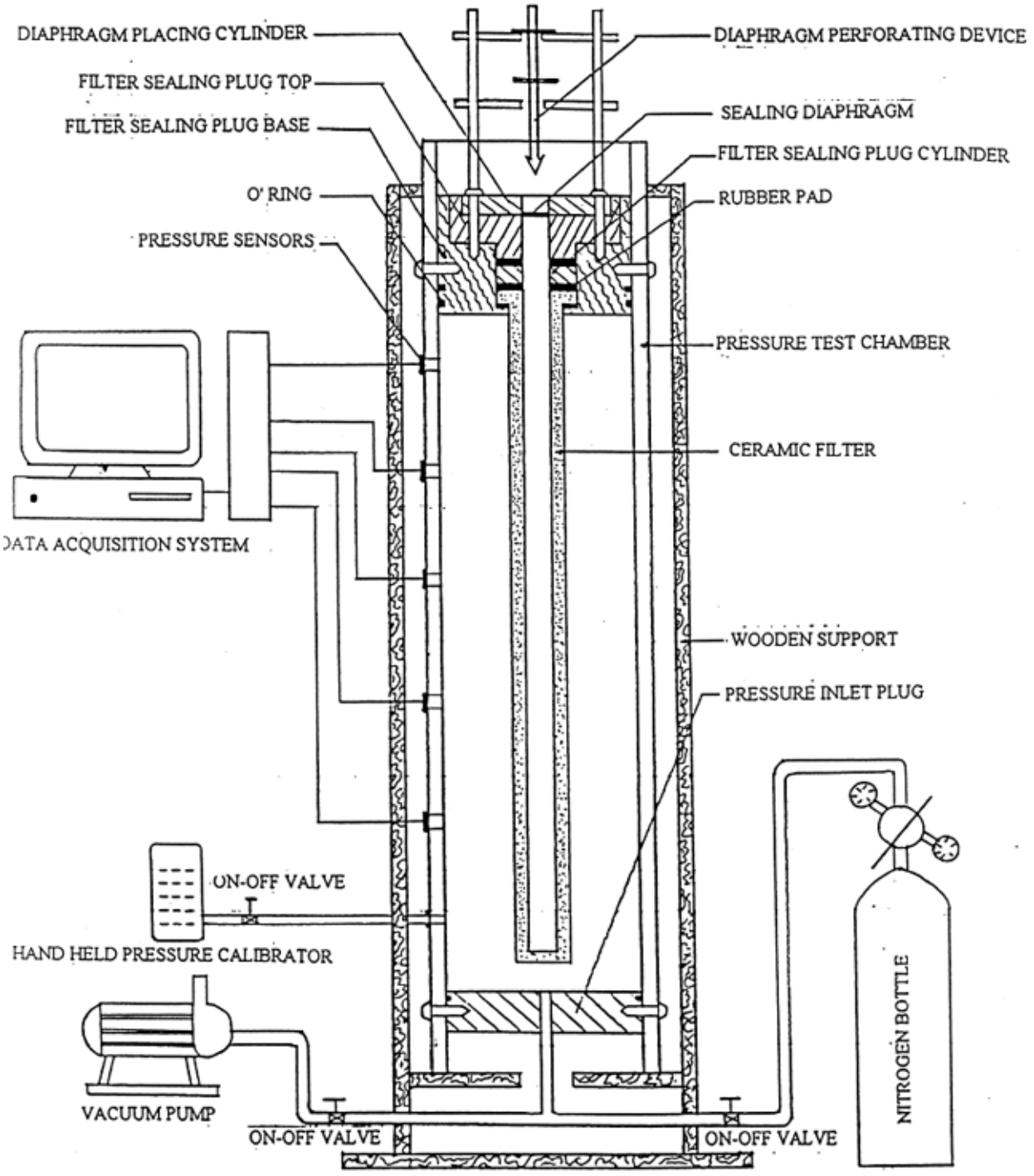

Figure 2-1-2 Schematic of filter test setup

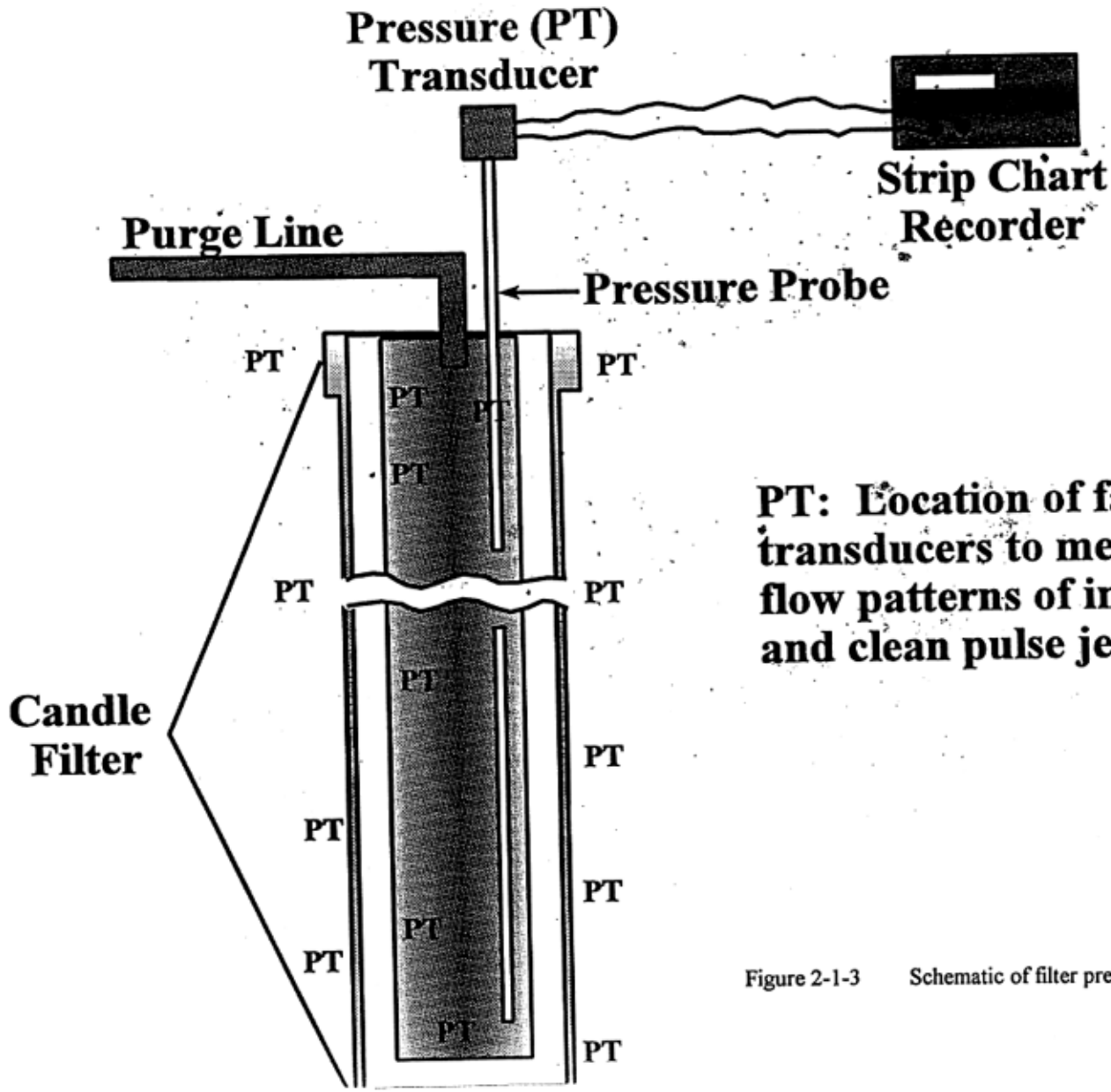

PT: Location of fast pressure transducers to measure the flow patterns of inlet, filtrated and clean pulse jets.

Figure 2-1-3 Schematic of filter pressure field test setup

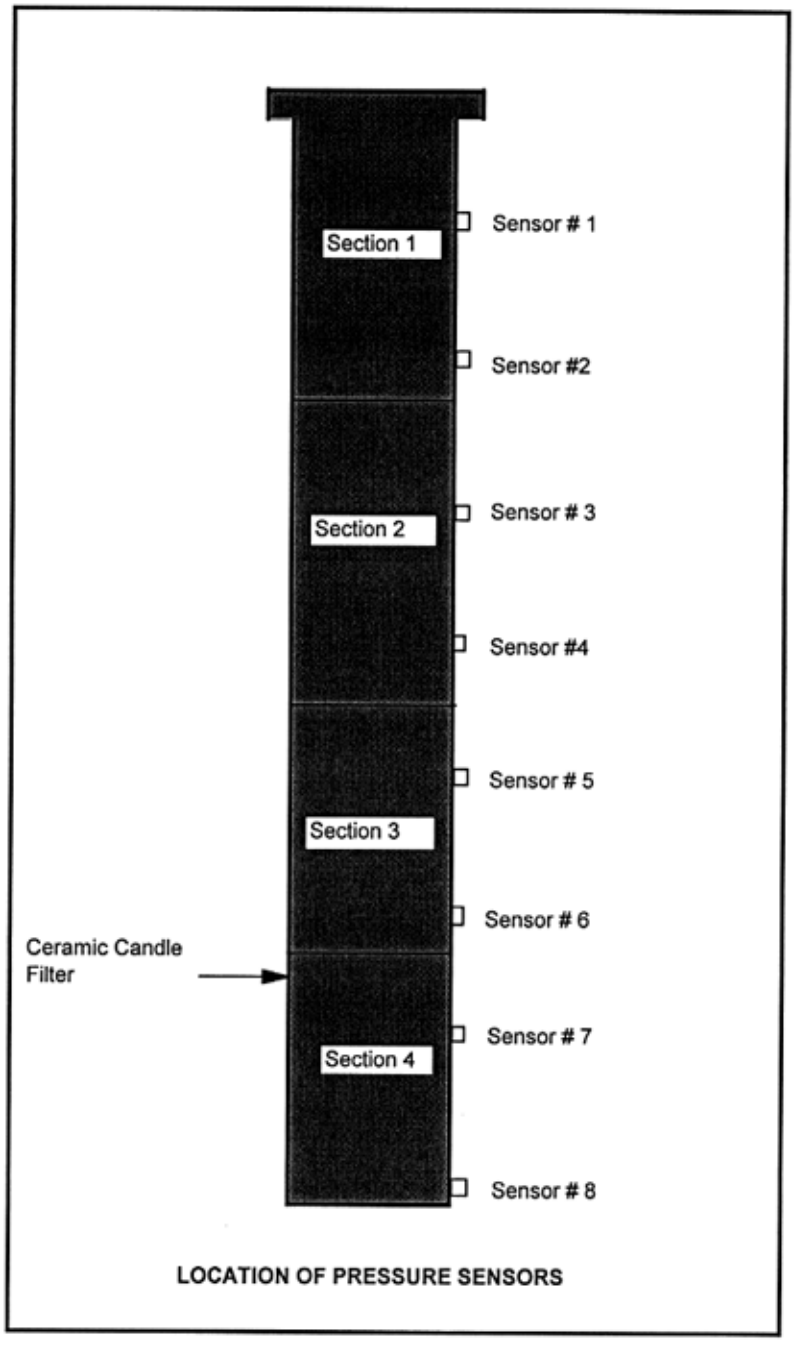

Figure 2-1-4 Schematic of section of filter and sensors location

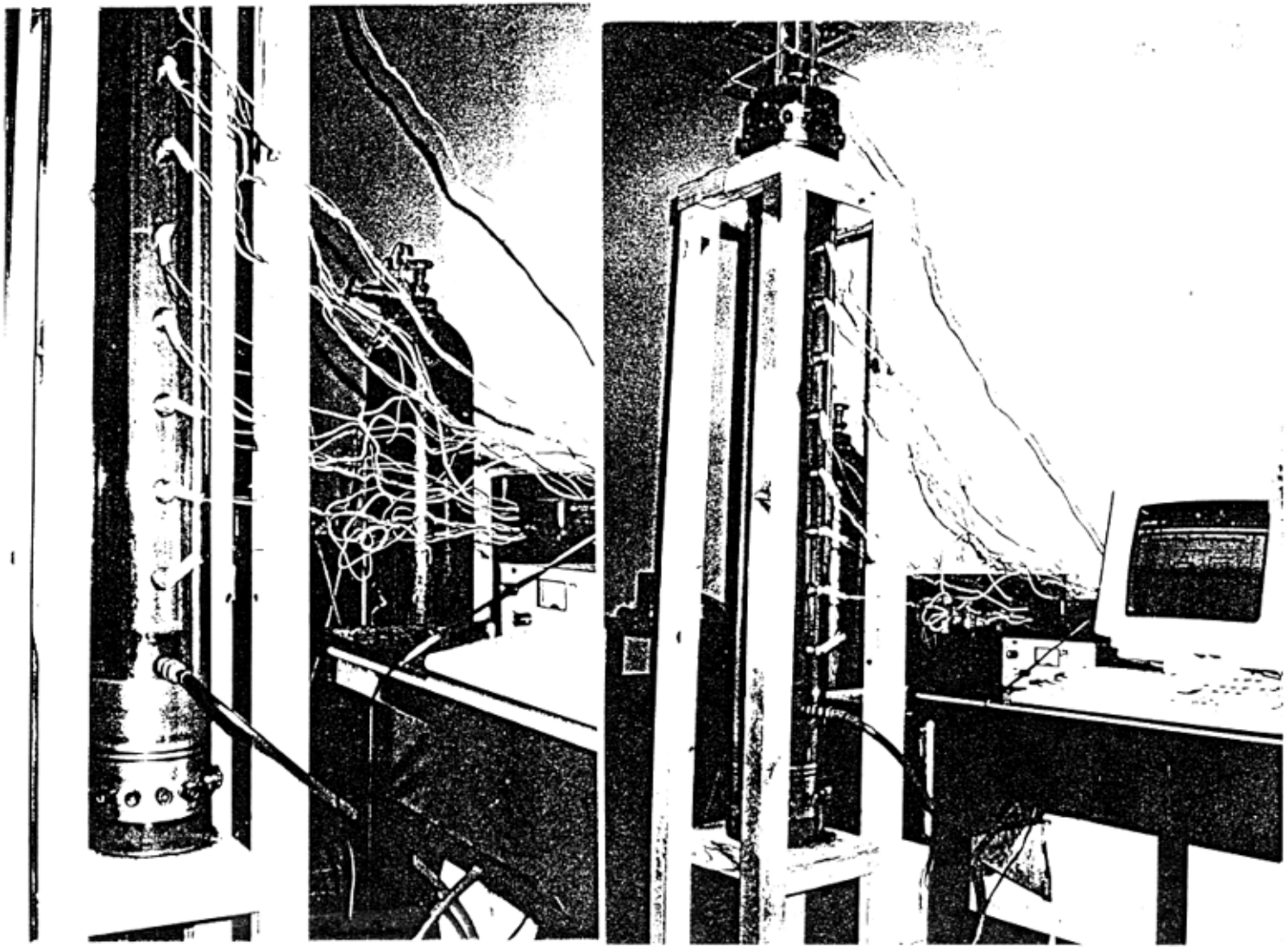

Figure 2-1-5 Picture of filter test setup

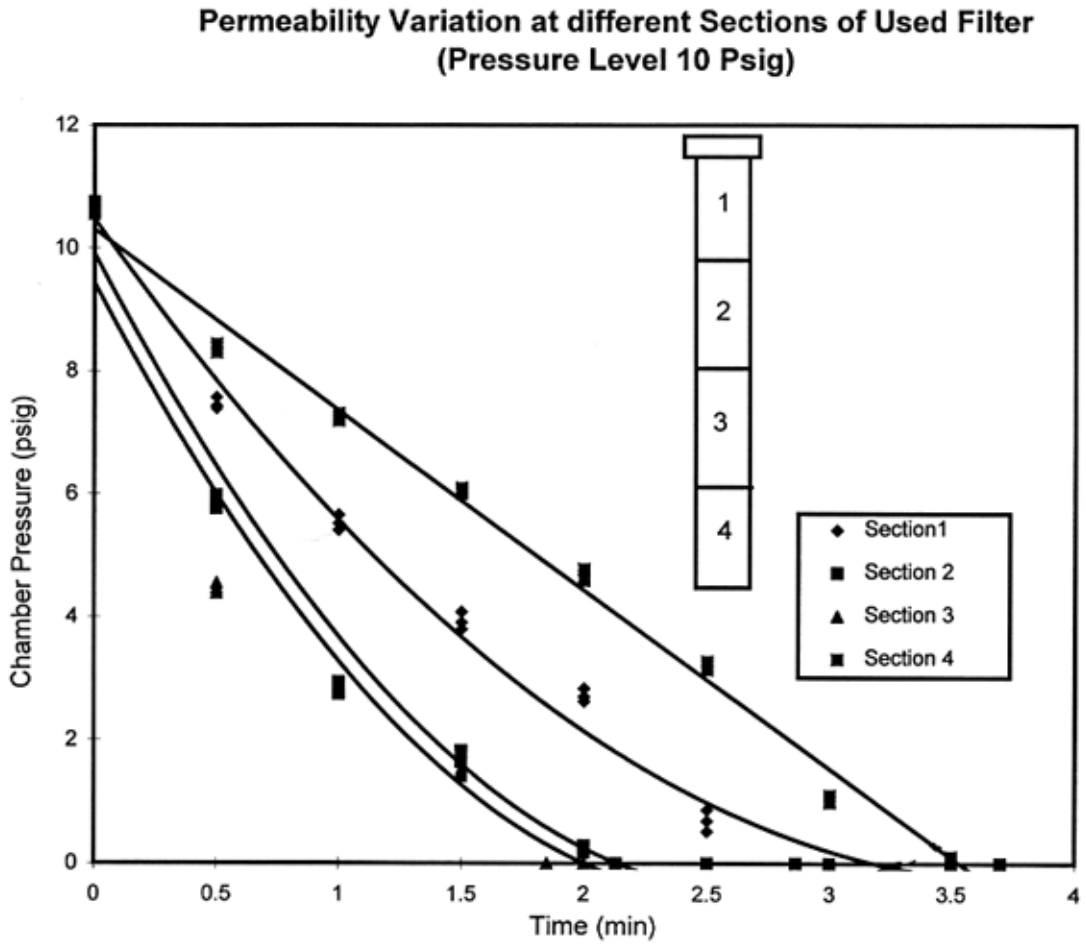

Figure 2-1-6 Permeability variation of used filter (10) psi

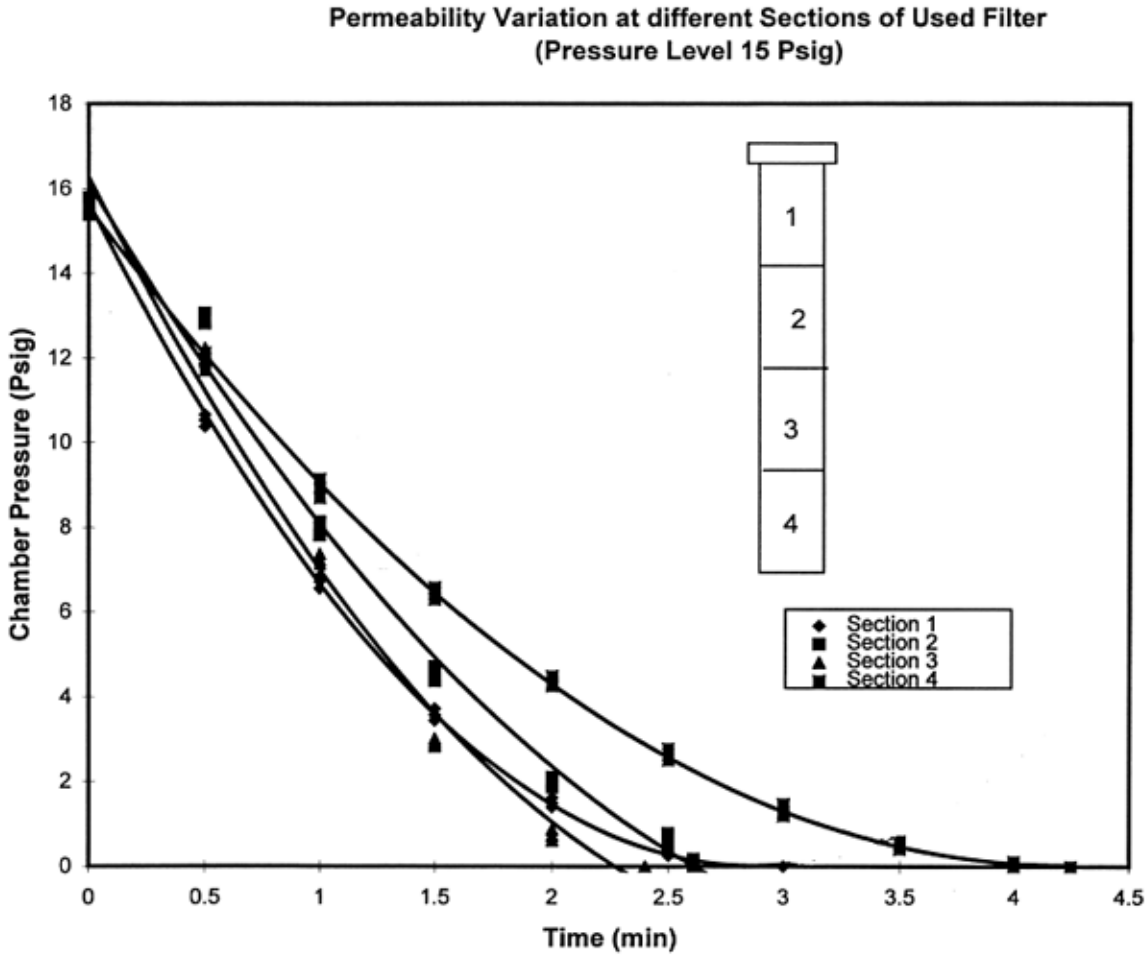

Figure 2-1-7 Permeability variation of used filter (15) psi

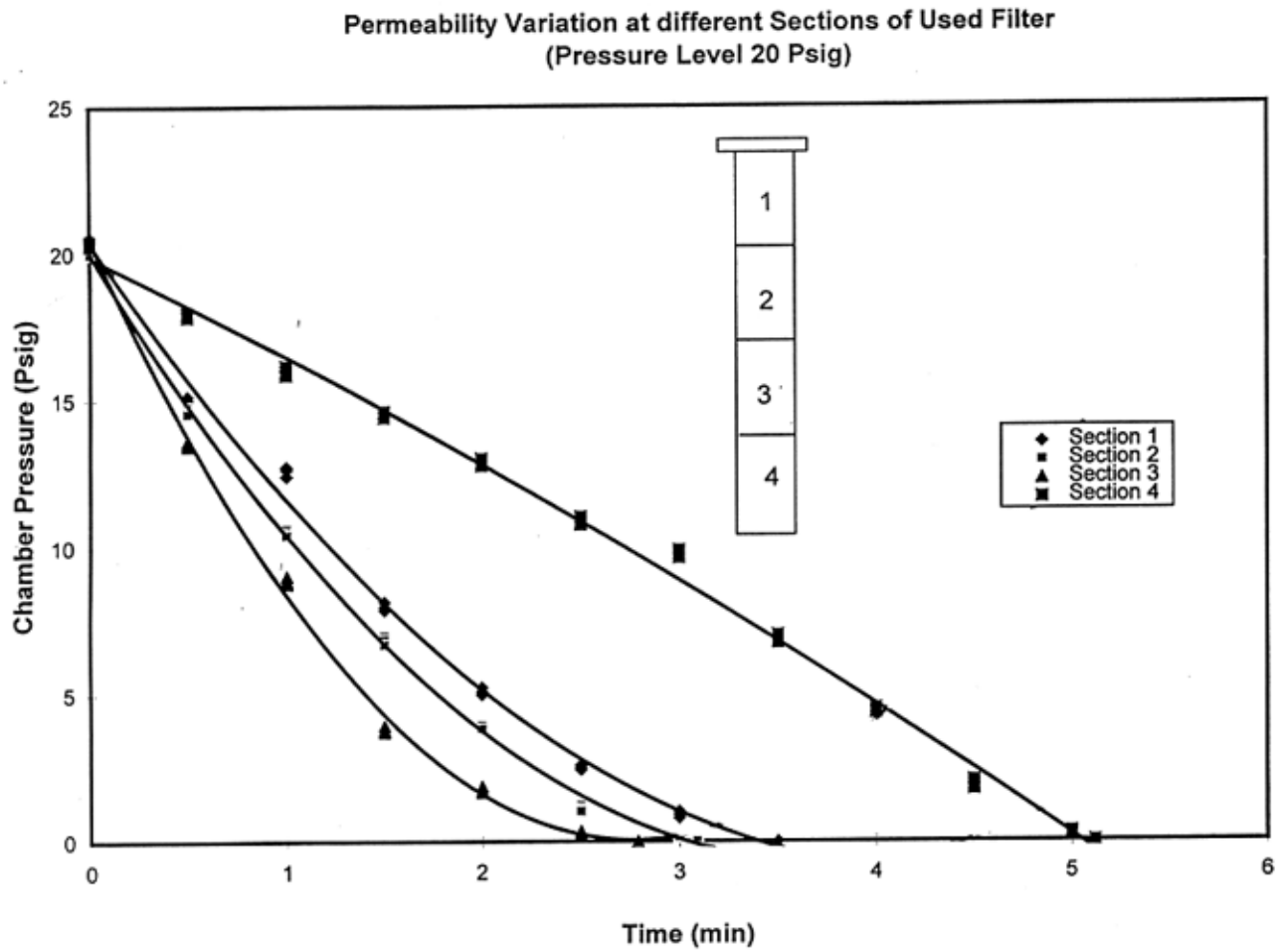

Figure 2-1-8 Permeability variation of used filter (20) psi

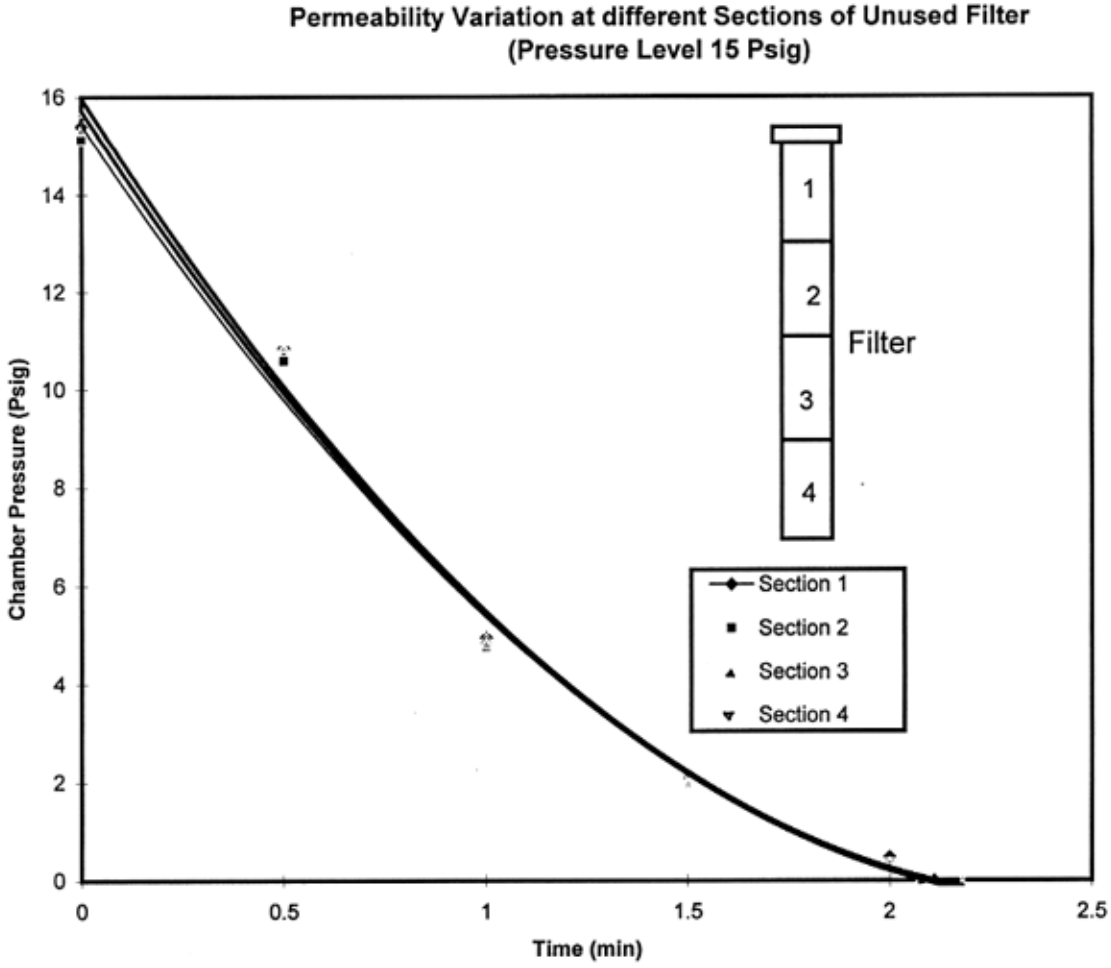

Figure 2-1-9(a) Permeability variation of unused filter (15) psi

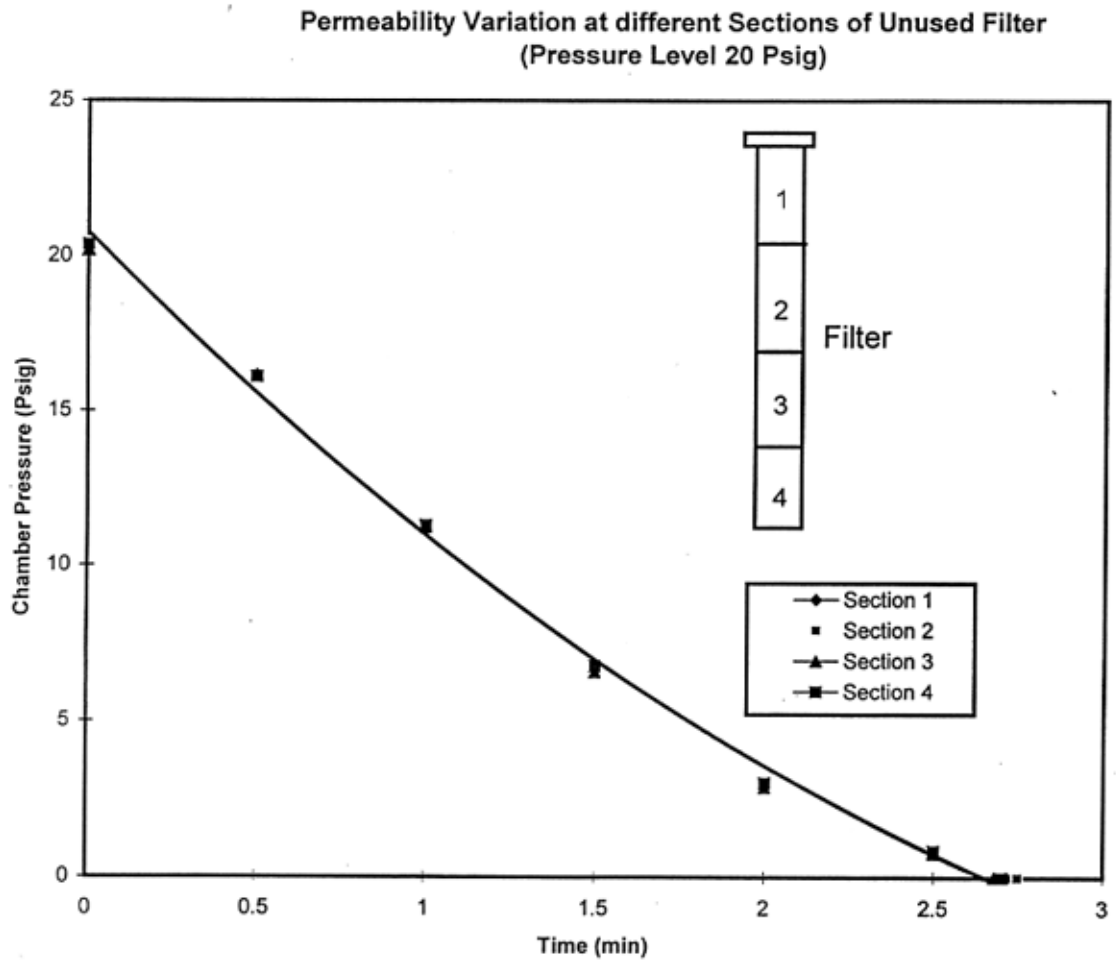

Figure 2-1-9(b) Permeability variation of unused filter (20) psi

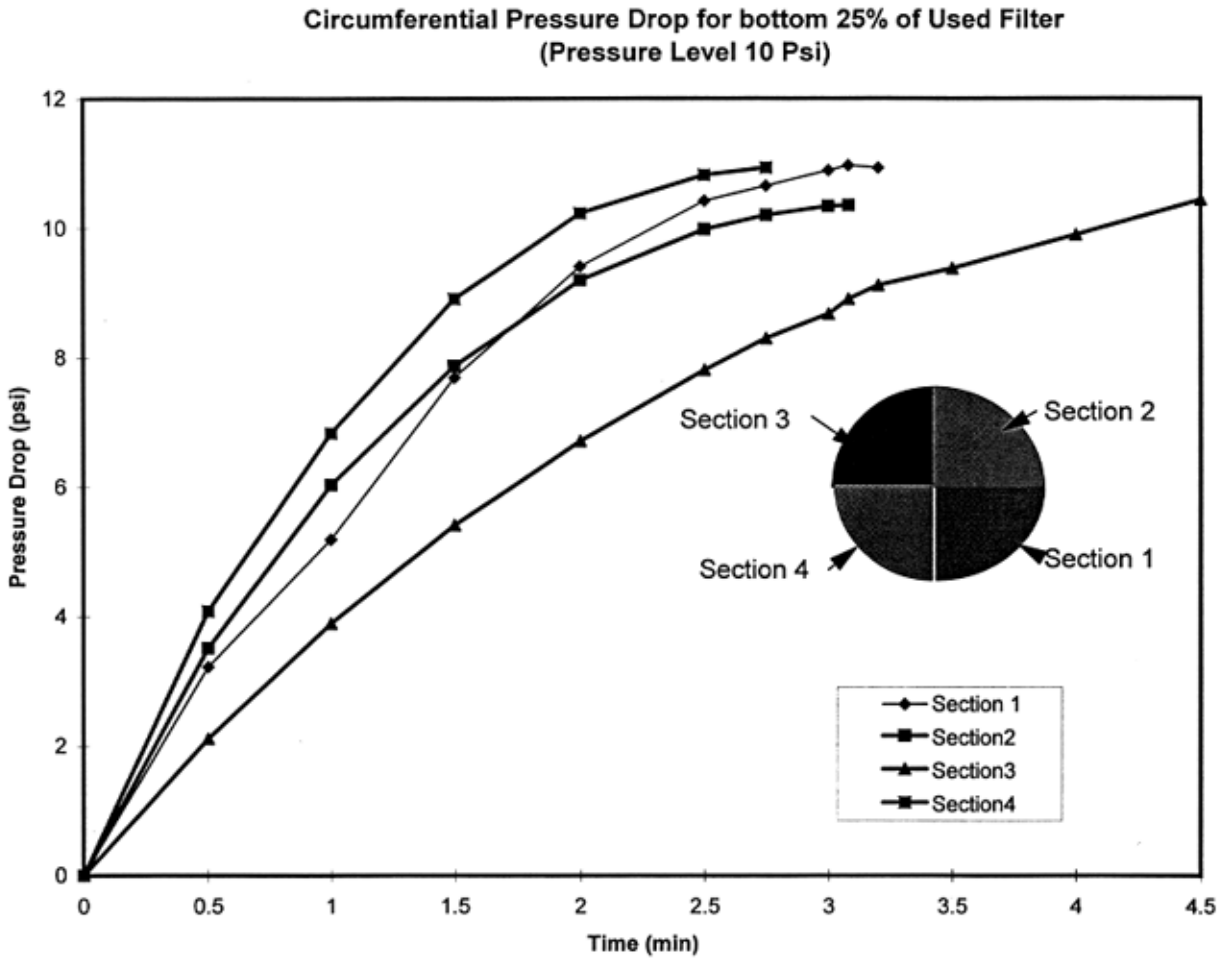

Figure 2-1-10 Permeability circumferential variation of used filter (10) psi

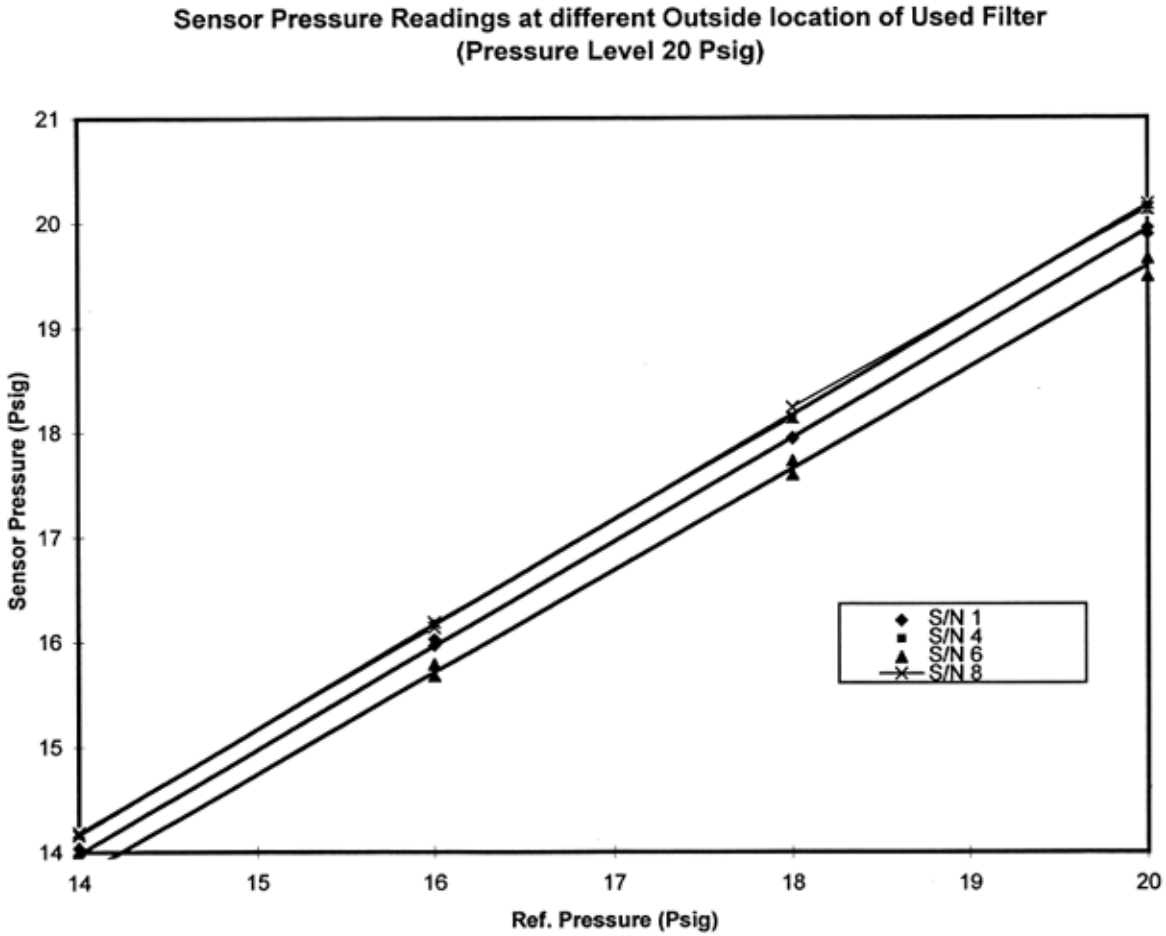

Figure 2-1-11 Pressure sensor output of used filter (20) psi, outside filter

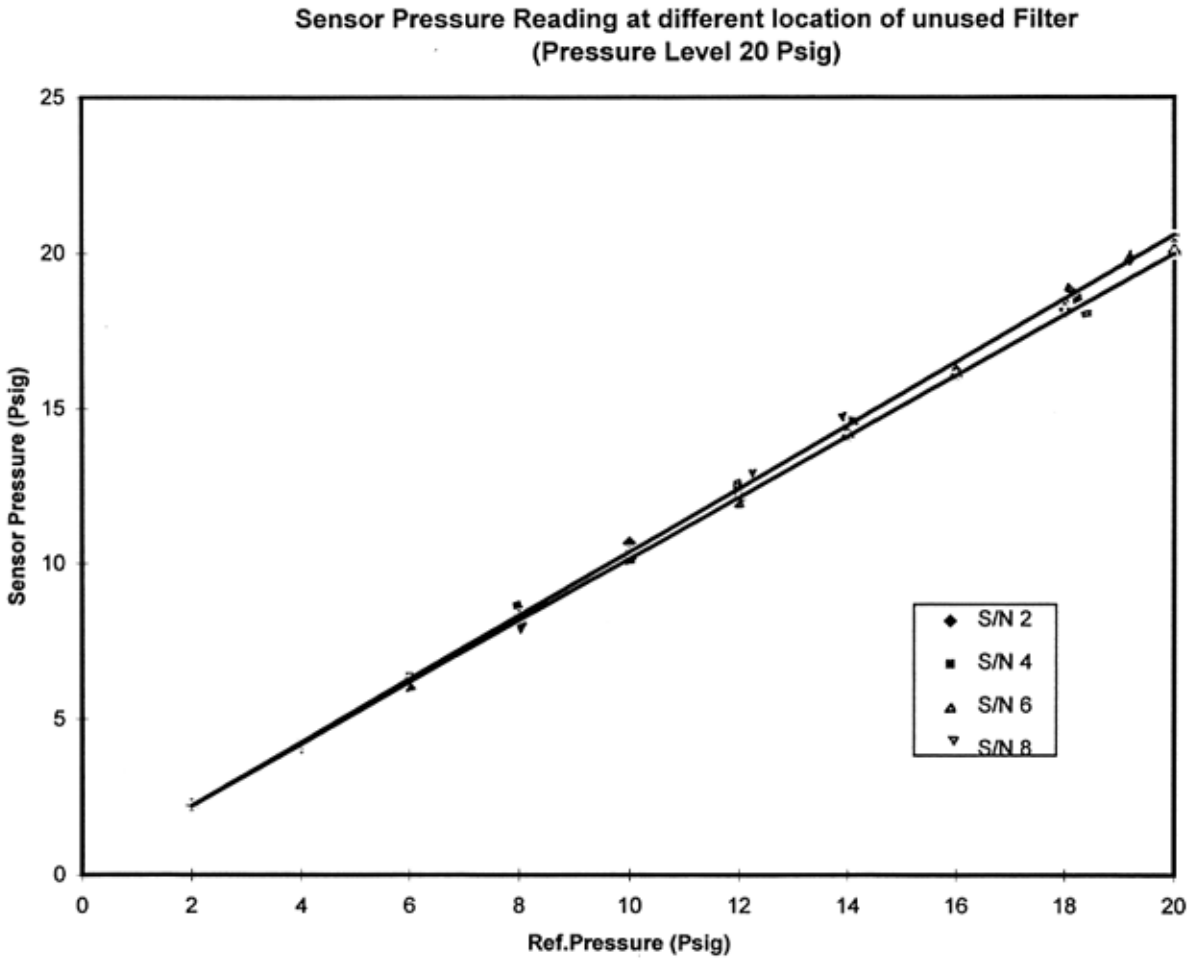

Figure 2-1-12 Pressure sensor output of unused filter (20) psi, outside filter

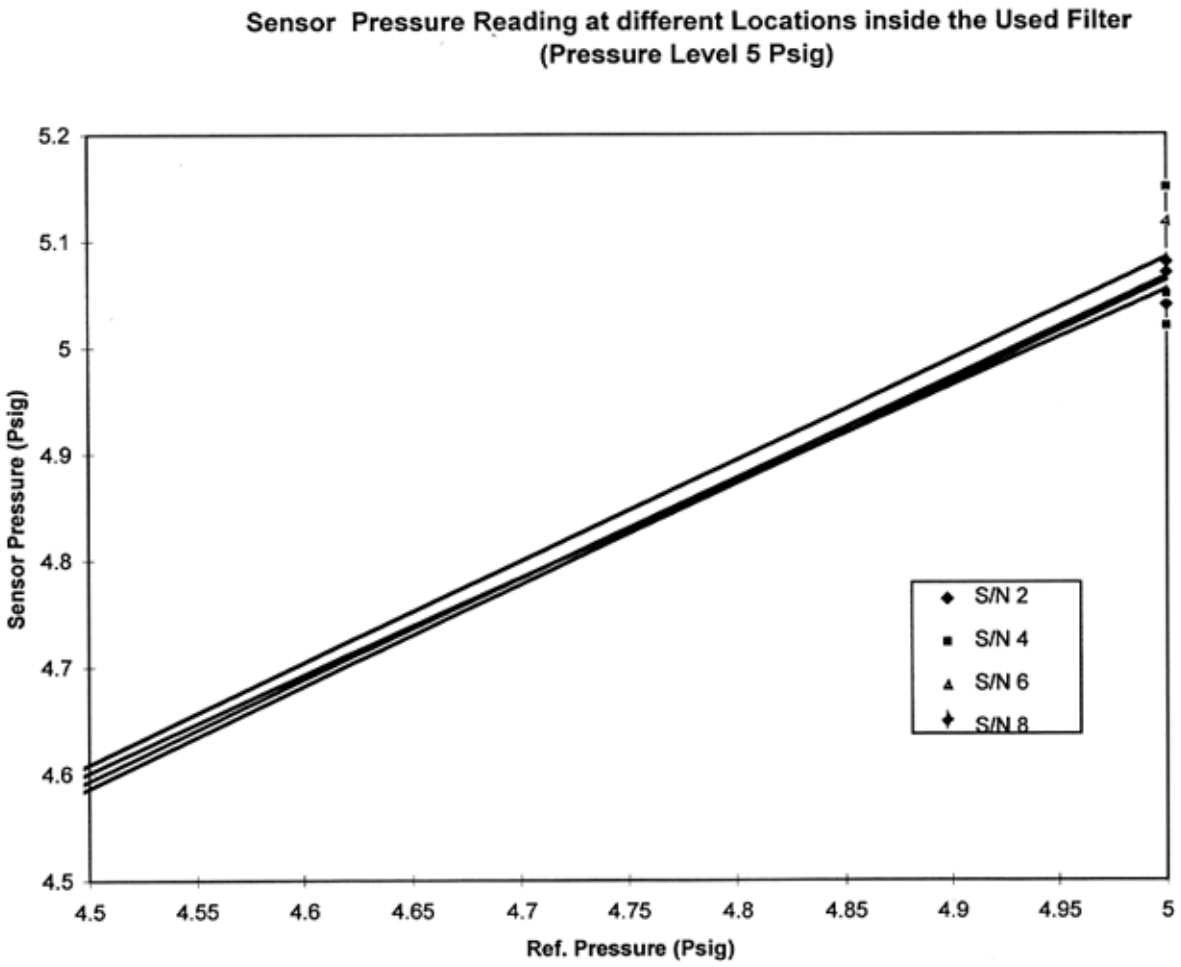

Figure 2-1-13 Pressure sensor output of used filter (5) psi, inside filter

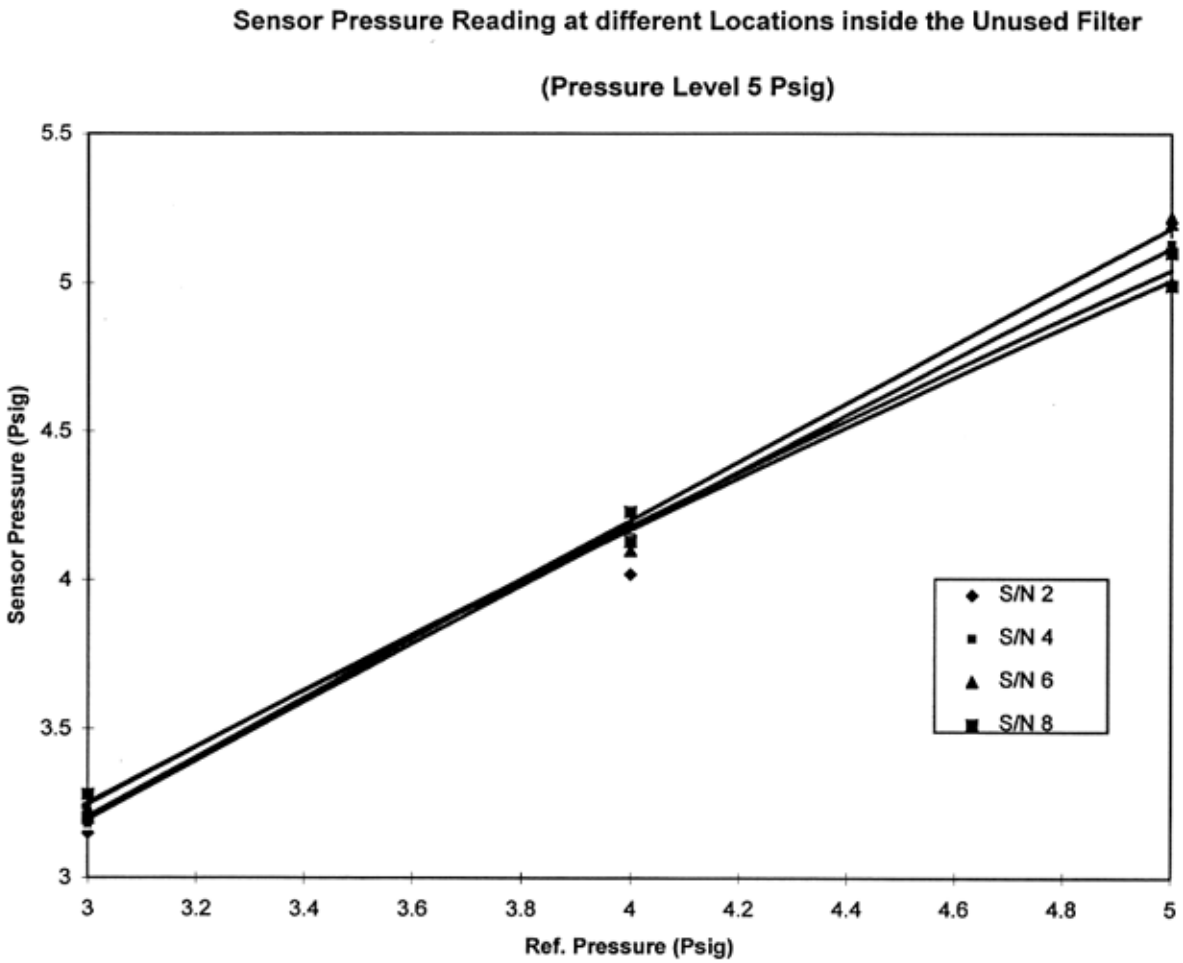

Figure 2-1-14 Pressure sensor output of unused filter (5) psi, inside filter

(a)

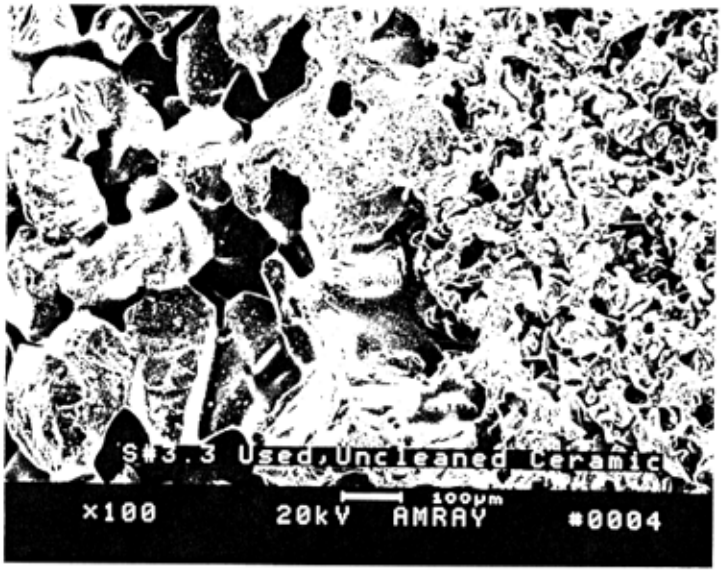

(b)

SEM Micrographs of: (a) unused; (b) used; (c) used and ultrasonically cleaned ceramic filters, illustrarting the double layer structures.

Figure 2-2-1 SEM micrographs of unused, used and ultrasonically cleaned filters

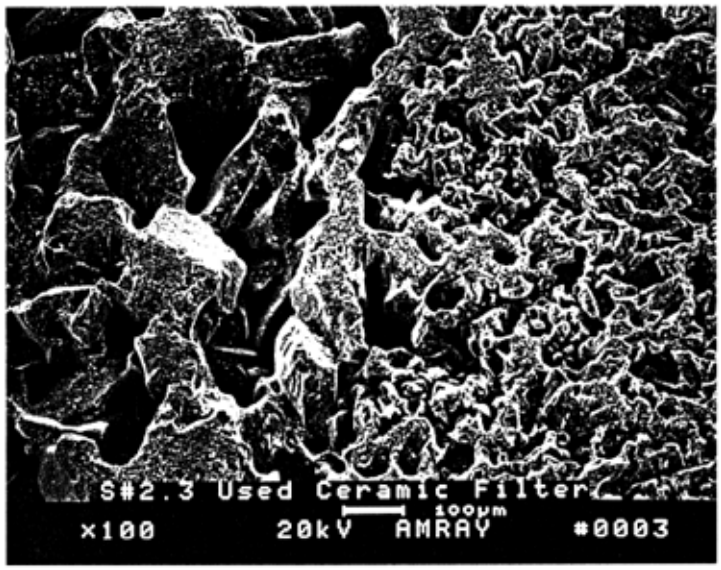

(c)

Figure 2-21-1 SEM Micrographs of the (a) unused (b) used and (c) used ultrasonically cleaned ceramic filters, illustrating the double layers structures.

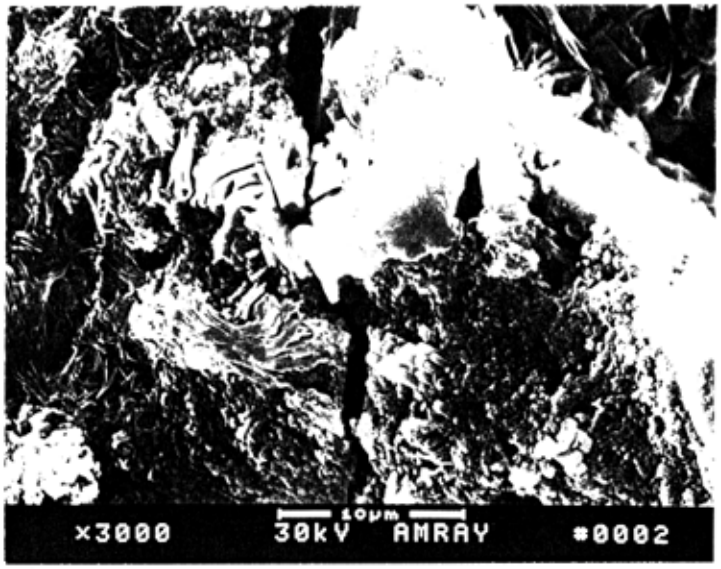

(a)

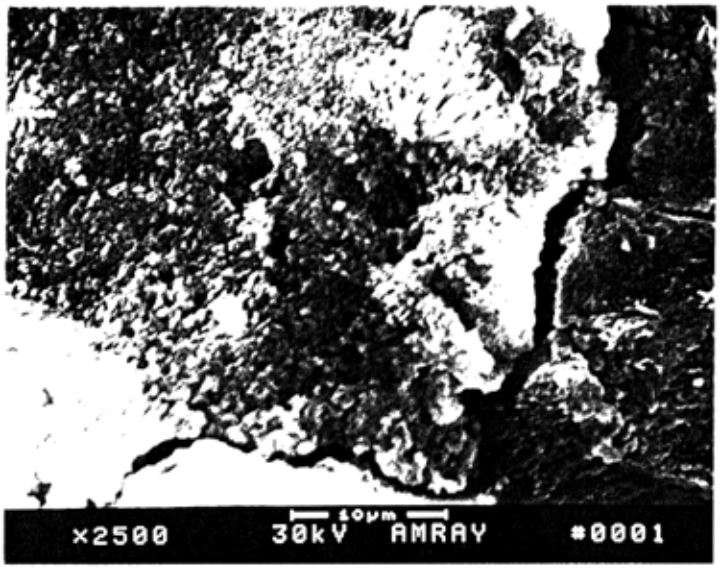

(b)

SEM micrographs of unstable cracks penetrating on: (a) the outer surface; and (b) inner surface of the used ceramic filter.

Figure 2-2-2 SEM micrographs of unstable cracks penetration on inner and outer filter surface

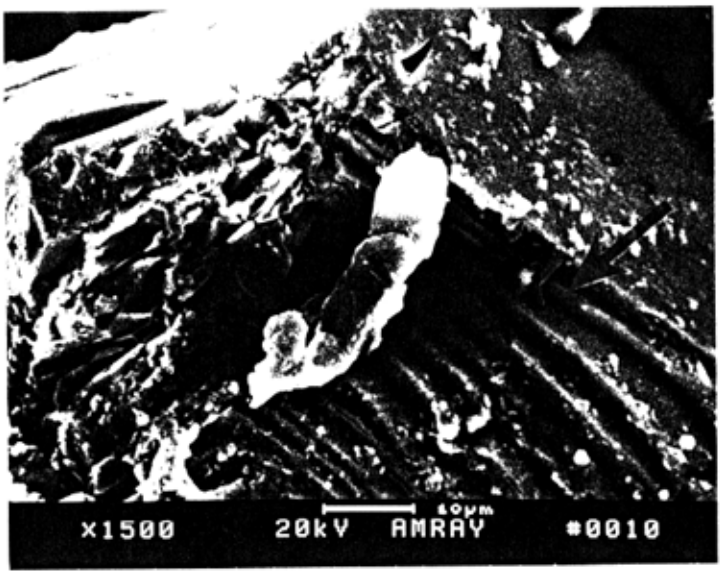

(a)

(b)

SEM micrographs of cleavage fracture "river marks" through the outer layer of the used ceramic filter caused by reverse pulse cleaning: (a) at 1500 X; and (b) at 6000 X.

Figure 2-2-3 SEM micrographs of the "river marks" through the outer layer of used filter

XPS spectra of the outer layer of the used and ultrasonically cleaned filter

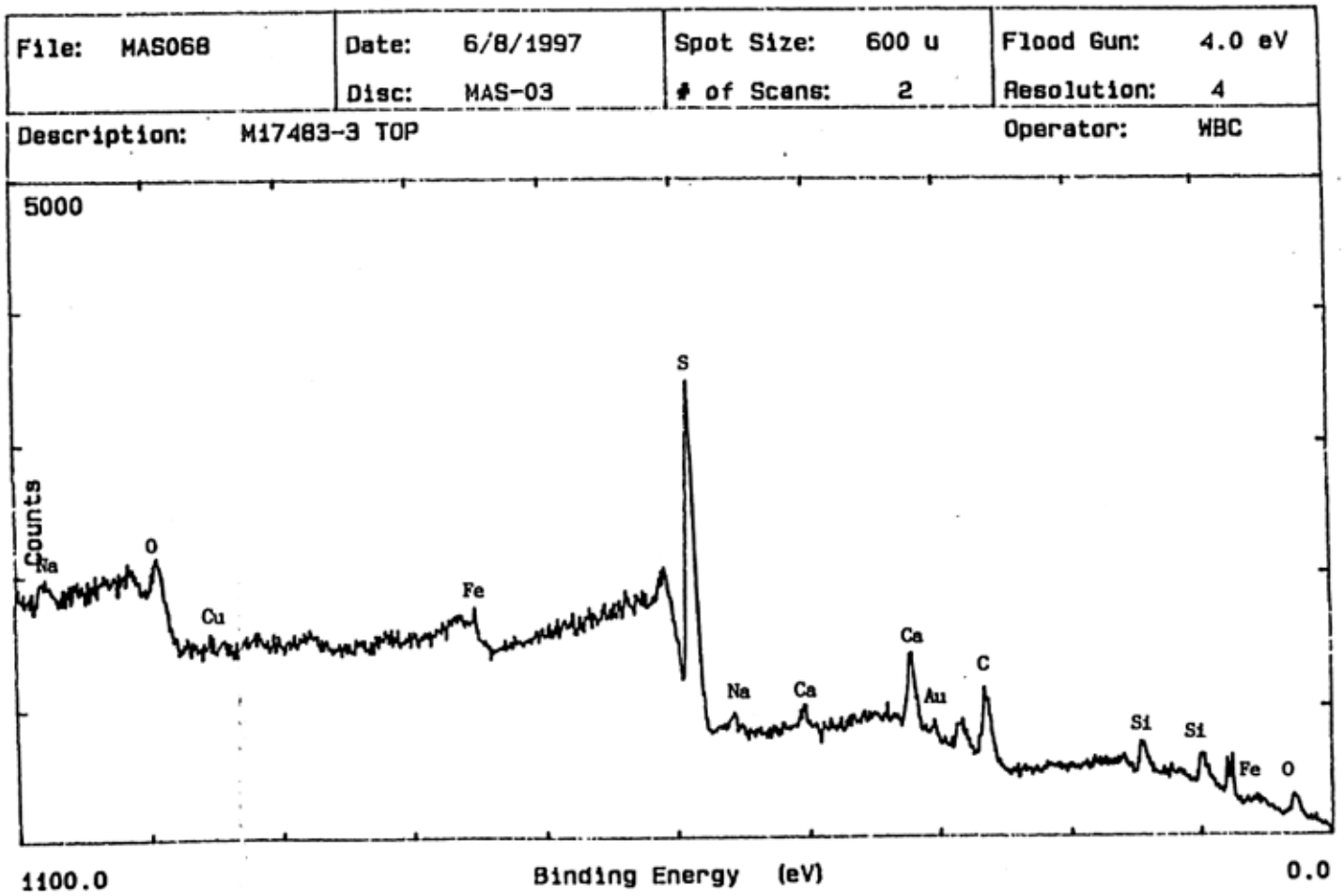

Figure 2-2-4 XPS spectra of the outer layer of the used ceramic filter cleaned ultrasonically, showing elements presented.

XRD spectra of the layer formed by depositions and reactions on used filter surface

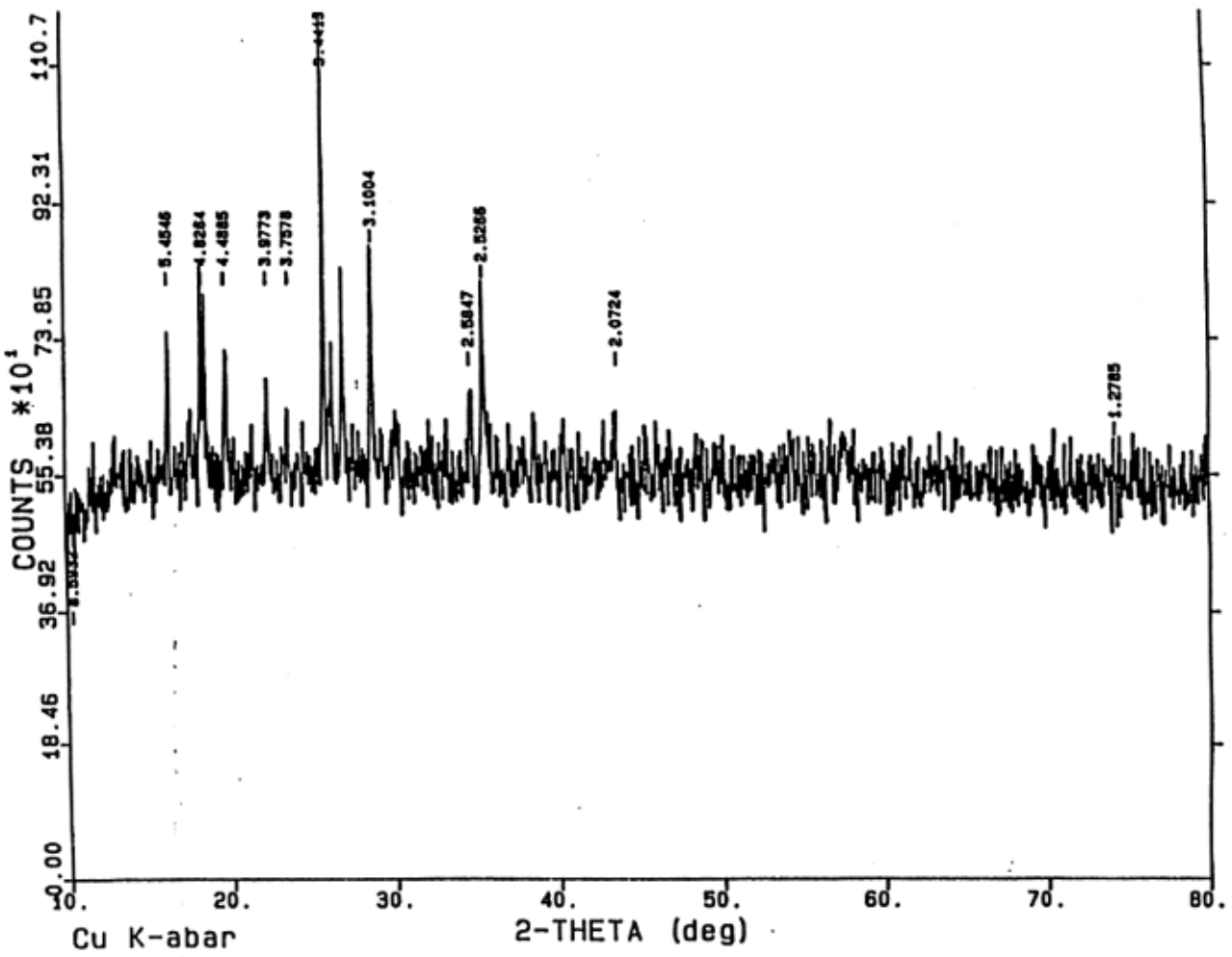

Figure 2-2-5 XRD spectra of the layer formed by depositions and reactions on the surface of the used ceramic filter.

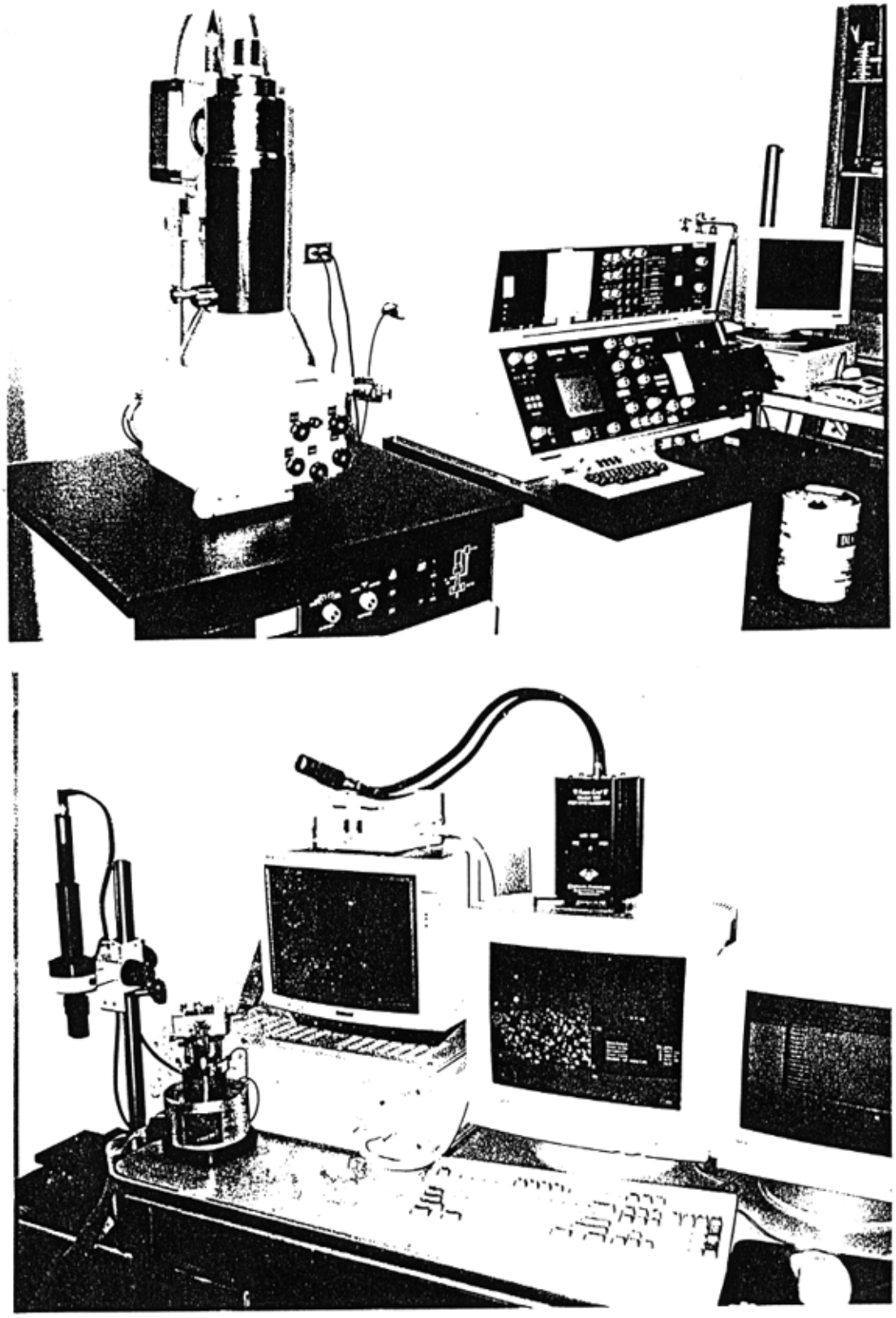

Figure 2-2-6 Picture of material laboratory analysis equipment

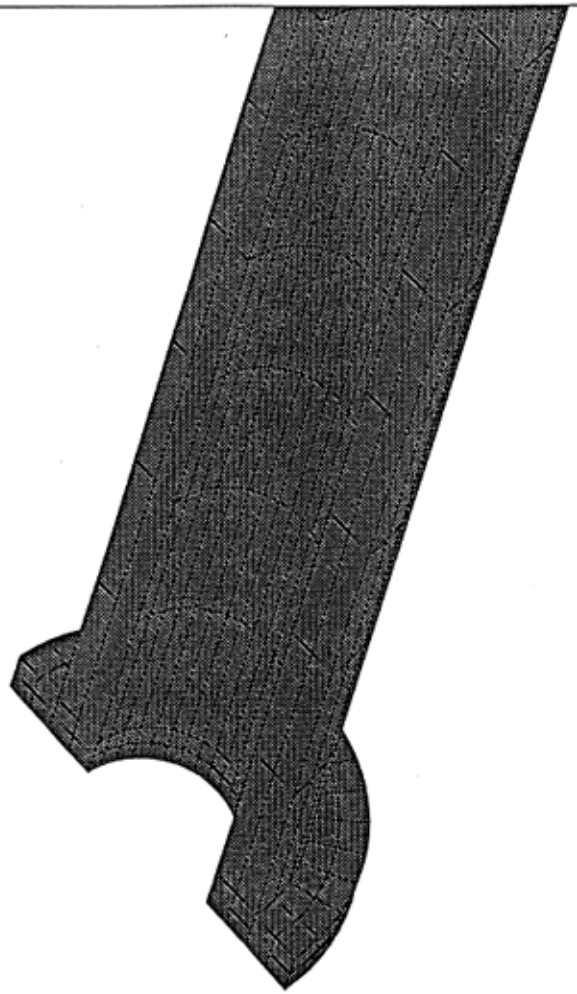

ANSYS 5.0 A 20
JUN 25 1996
18:10:15
PLOT NO. 1
ELEMENTS
TYPE NUM

XV =-0.298836
YV =-0.429547
ZV =-0.852166
*DIST=0.131514
*XF =-0.168714
*YF =-0.246198
*ZF =0.956467
A-ZS=-56.38
CENTROID HIDDEN

Figure 2-3-1 FEA model on filter back pulse cleaning near the neck with element meshing

Figure 2-3-2 Picture of FEA model on back pulse cleaning near the neck with element meshing

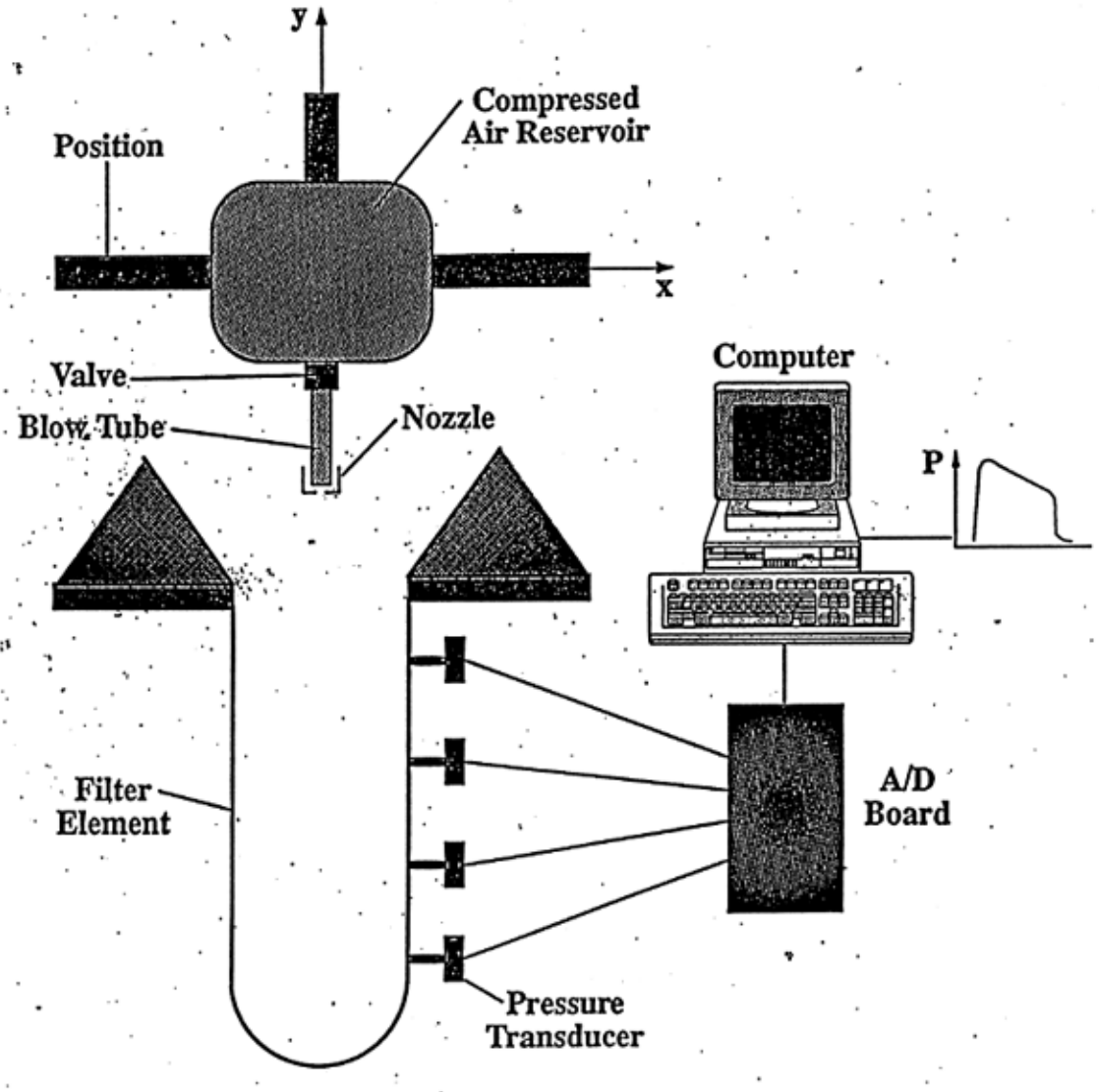

Figure 2-4-1 Schematic of test setup configuration for parametric study on filtration process

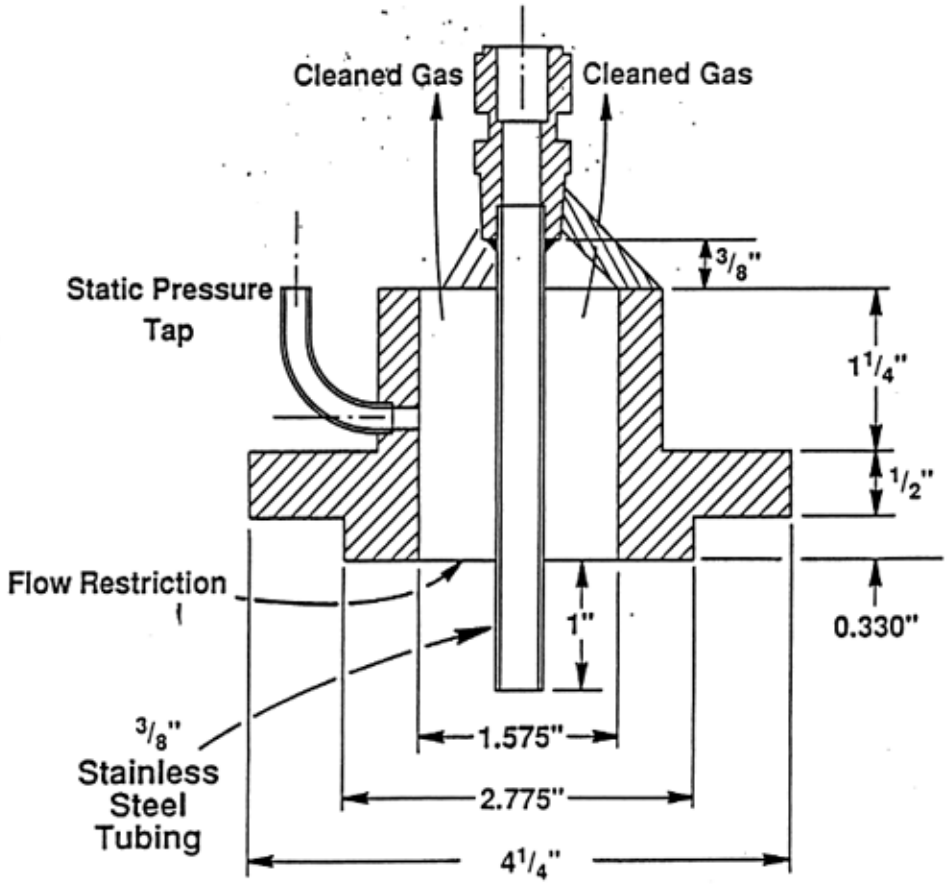

Figure 2-4-2 Configuration of back pulse gas stream setup for dust cake dislodging